nature communications

Article

https://doi.org/10.1038/s41467-024-52738-z

A specific folate activates serotonergic neurons to control *C. elegans* behavior

Received: 28 November 2023

Accepted: 19 September 2024

Published online: 30 September 2024

Check for updates

Ria S. Peesapati[1,3], Brianna L. Austin-Byler[1,3], Fathima Zahra Nawaz[1], Jonathan B. Stevenson[1], Stanelle A. Mais[1], Rabia N. Kaya[1], Michael G. Hassan[1], Nabraj Khanal[1], Alexandra C. Wells[1], Deena Ghiai[1], Anish K. Garikapati[1], Jacob Selhub[2] & Edward T. Kipreos[1]

Folates are B-group vitamins that function in one-carbon metabolism. Here we show that a specific folate can activate serotonergic neurons in *C. elegans* to modulate behavior through a pathway that requires the folate receptor FOLR-1 and the GON-2 calcium channel. FOLR-1 and GON-2 physically interact in a heterologous system, and both are expressed in the HSN and NSM serotonergic neurons. Both the folate 10-formyl-THF and a non-metabolic pteroate induce increases in the number of Ca^{2+} transients in the HSN neurons and egg laying in an FOLR-1- and GON-2-dependent manner. FOLR-1 and GON-2 are required for the activation of the NSM neurons in response to 10-formyl-THF, and for full NSM-mediated stoppage of movement when starved animals encounter bacteria. Our results demonstrate that FOLR-1 acts independently of one-carbon metabolism and suggest that 10-formyl-THF acts as a dietary signal that activates serotonergic neurons to impact behavior through a pathway that involves calcium entry.

Folates are a family of related molecules that function in one-carbon metabolism[1]. Folates are comprised of three structural moieties: a pteridine ring; para-aminobenzoic acid, and one or more glutamate residues[1] (Supplementary Fig. 1a). Folates contribute or accept one carbon unit during the one-carbon metabolism cycle. This process of gaining or losing one carbon unit interconverts folates between types (Supplementary Fig. 1b). The addition of one carbon units to substrates generate: the purine precursors 5-phosphoribosyl-*N*-formylglycinamide and 5-formaminoimidazole-4-carboxyamide ribotide; deoxythymidine monophosphate; and methionine[2]. Additionally, serine and glycine are interconverted by the addition or removal of a one-carbon unit, respectively[2].

There are three major classes of folate transporters: the reduced folate carrier, which mediates the majority of folate transport into most animal cells; the proton-coupled folate transporter, which mediates the transport of folate in the mammalian intestine; and the folate receptor (FOLR)[3].

The FOLR is a high-affinity, low-throughput folate transporter. In mammals, FOLR-1 functions in the transcytosis of folates across cell barriers (e.g., in the choroid plexus to cross the blood-brain barrier, in the placenta to transport folates from mother to embryo, and in the kidney to bring folate in pre-urine back into the body)[4–6]. The mammalian folate receptor FOLR1 is not expressed at detectable levels in many tissues but is overexpressed in multiple types of cancers[7]. Heightened expression of FOLR1 increases cancer progression and worsens patient prognosis in several of these cancers[7].

C. elegans contains one folate receptor, FOLR-1, that is evolutionarily related to the four FOLRs in mammals. We had previously shown that FOLR-1 functions in a pathway to increase the rate of proliferation of *C. elegans* germ stem cells above basal levels in response to a specific folate, 10-formyl-tetrahydrofolate (10F-THF), that is obtained from the bacterial diet[8].

While germ cells in *C. elegans* respond to 10F-THF to increase their proliferation rate above basal levels, they do not respond in a similar

[1]Department of Cellular Biology, The University of Georgia, Athens, GA, USA. [2]Jean Mayer USDA Human Nutrition Research Center on Aging, Tufts University, Boston, MA, USA. [3]These authors contributed equally: Ria S. Peesapati, Brianna L. Austin-Byler. e-mail: ekipreos@uga.edu

manner to other folates that function in one-carbon metabolism (5-methyl-THF, 5-formyl-THF, and THF)[8]. Notably, 5-formyl-THF can rescue folate deficiency better than 10F-THF[8]. However, unlike 10F-THF, 5-formyl-THF does not increase germ cell proliferation above basal levels, suggesting a decoupling of the role of folates in metabolism from the pathway that increases germ cell proliferation above basal levels[8]. Notably, FOLR-1 is not required for basal germ cell proliferation. However, FOLR-1 is required for the increased rate of germ cell proliferation in response to 10F-THF[8].

Several lines of evidence indicate that the regulation of germ cell proliferation by 10F-THF occurs independently of metabolism[8]. The most direct evidence is that the FOLR-1-dependent increase in germ cell proliferation can be stimulated by a pteroate, which cannot be used in one-carbon metabolism[9]. Pteroates are structurally similar to folates but lack glutamic acid residues (Supplementary Fig. 1a). The conversion of the pteroate dihydropteroate (DHP) to dihydrofolate (DHF) by the addition of a glutamyl moiety is the last step in folate synthesis in bacteria, fungi, and plants, and is catalyzed by the enzyme DHF synthase (Supplementary Fig. 1a)[10]. All animals, including nematodes, lack DHF synthase, and, therefore, cannot synthesize folates[9,10]. Similarly, the bacteria *Lactobacillus casei* does not have functional DHF synthase, and so cannot synthesize folates[9]. *L. casei* is used in a biological assay for folate levels because they grow equally well when provided with any of the different types of folate. *L. casei*, however, cannot grow when provided pteroates. This is because *L. casei* cannot use pteroates for one-carbon metabolism and cannot convert pteroates to folates[9]. Similarly, animals cannot utilize pteroates for one-carbon metabolism or convert them to folates because they lack DHF synthase[9]. Consistently, we have observed that folate deficiency in *C. elegans* cannot be rescued by providing the pteroate DHP, but can be rescued by providing various individual folate types[8]. Despite not functioning in one-carbon metabolism, pteroates can bind to mammalian FOLR1 with high affinity[11]. Thus, the observation that a pteroate can stimulate increased germ cell proliferation through a FOLR-1-dependent pathway implies that the pathway functions independently of one-carbon metabolism. Here we will demonstrate a metabolism-independent role for FOLR-1 in the activation of serotonergic neurons to regulate behavior.

In *C. elegans*, there are four types of neurons that synthesize serotonin (5-hydroxytryptamine, 5-HT), with two neurons per type[12]. Two of these serotonergic neuron types, HSN and NSM, regulate behavior in response to ingested bacteria. One serotonergic neuron type, ADF, regulates movement in response to volatile bacterial chemotaxis signals[13], and the serotonergic neuron type VC4/5 functions with HSN to promote the laying of eggs (i.e., embryos encased in an eggshell)[14,15].

The two hermaphrodite-specific motor neurons (HSNR and HSNL) are located bilaterally near the vulva (Fig. 1a). The HSN neurons form synapses with the vulval muscles and ventral cord neurons[14]. HSN is responsible for modulating the timing of egg laying[14,15], which is stimulated in response to ingested bacteria[16,17]. If the HSN neurons are ablated, the timing between egg-laying events is substantially lengthened and hermaphrodites accumulate excessive numbers of unlaid eggs[17].

The two neurosecretory NSM neurons (NSML and NSMR) are located in the pharynx, which is an organ composed of non-striated muscle that ingests and crushes bacteria for digestion (Fig. 1a). The NSM neurons are required for a stopping behavior in which starved animals stop their forward motion when ingesting bacteria[13,18,19]. NSM mediates this behavior through the systemic release of serotonin, which is bound by receptors on body-wall muscles, causing them to stop their contractions[13,18,19]. NSM also contributes to a dwelling behavior in which fed animals have reduced movements for periods of time[20].

Results

FOLR-1 is expressed in HSN and NSM neurons

In an effort to understand the cellular and organismal roles of *C. elegans* FOLR-1, we determined the expression pattern of a transgene in which FOLR-1 is fused to a C-terminal GFP and expressed under the regulation of its own promoter (*folr-1p*). The *folr-1p*::FOLR-1::GFP transgene is expressed in a relatively small subset of cells in the soma of larvae and adults, including several neurons in the head and two neurons in the midsection, cells in the tail, the pharyngeal-intestinal valve (vpi) cells that link the pharynx to the intestine, and the isthmus of the pharynx (Fig. 1a, b, and d, and Supplementary Figs. 2 and 3a). There is also transient expression in uterine cells during the late L4 and young adult stages (Supplementary Fig. 3b).

The *folr-1p*::FOLR-1::GFP expression pattern includes the two NSM serotonergic neurons (Fig. 1a, b). This was confirmed by observing the overlapping expression of the *folr-1p*::FOLR-1::GFP transgene with mCherry expressed using the *tph-1p* promoter (Supplementary Fig. 2). The *tph-1* gene encodes tryptophan hydroxylase, which is required for the synthesis of serotonin, and is a marker for serotonergic neurons, including NSM and HSN[12]. It is difficult to assess the expression of *folr-1p*::FOLR-1::GFP in the NSM neurites because the neurites extend into the isthmus of the pharynx, which also has FOLR-1::GFP expression (Fig. 1a, b). To visualize the NSM neurites without background staining, we expressed FOLR-1::wrmScarlet using a truncated *tph-1* promoter (*tph-1pDE*) that is specific for NSM expression[21]. The NSM neurites were visualized by expressing myristoylated mNeonGreen (myr-mNeonGreen), which is membrane localized. We observed that FOLR-1 is localized to the NSM cell body and its two major neurites but was absent from the thin minor neurite (Fig. 1c). Lower exposures and the use of confocal microscopy show that FOLR-1 is expressed in NSM neurons in regions that are coincident with the plasma membrane (marked by myr-mNeonGreen), as expected for a plasma membrane-localized protein (Supplementary Fig. 4).

The *folr-1p*::FOLR-1::GFP transgene is also expressed in the two serotonergic HSN neurons. Confirmation that FOLR-1 is expressed in the HSN neurons was obtained by observing co-expression of *folr-1p*::FOLR-1::GFP with the red fluorescent protein DsRed expressed using the *tph-1* promoter, which is expressed in HSN[12] (Fig. 1d). The FOLR-1::GFP expression is present in the region of the HSN axons that extend from the cell body to the post-synaptic terminus with the vulva muscles.

FOLR-1 promotes egg laying in response to the folate 10F-THF

In order to assess the role of FOLR-1 in the HSN neurons, we created a null allele of the *folr-1* gene using CRISPR/Cas9 to cut within the second exon of *folr-1*. The *folr-1(ek44)* allele has a 13 base pair deletion in the second exon (Supplementary Fig. 5a). The *ek44* deletion introduces a frameshift after residue 87, which extends the protein for 24 out-of-frame amino acids before it truncates on a stop codon (Supplementary Fig. 5b). The *folr-1(ek44)* allele is thus predicted to lose 69% of the C-terminus of the wild-type FOLR-1 protein, including residues predicted to bind folate (based on alignment with the human FOLR1 protein). Additionally, nonsense-mediated decay is expected to reduce the level of *folr-1* mRNA[22]. Consistently, we observe that *folr-1(ek44)* mutants have *folr-1* mRNA levels that are 1/15th that of wild type (Supplementary Fig. 6).

Given that FOLR-1 is expressed in the HSN neurons, we wanted to determine whether the addition of folate impacts egg laying through the folate receptor. To test this, we starved adult hermaphrodites for 30 min by washing sequentially three times in M9 buffer. The starved hermaphrodites were placed on 6 cm plates that had 25 µl of 10 µM 10F-THF spread onto the plates a few minutes beforehand. The concentration of 10F-THF on the surface of the plate was estimated based on the diffusion of the dye bromophenol blue (see "Methods"). While the diffusion of bromophenol blue may not be equivalent to that of 10F-THF, the estimate of the surface concentration of 10F-THF based on that diffusion is: 70.6 ± 0.002 (SEM) nM at time 0 (when the animals initially contact the plate); 54.5 ± 0.0016 nM at 10 min; and 38.5 ± 0.0013 nM at 60 min.

https://doi.org/10.1038/s41467-024-52738-z

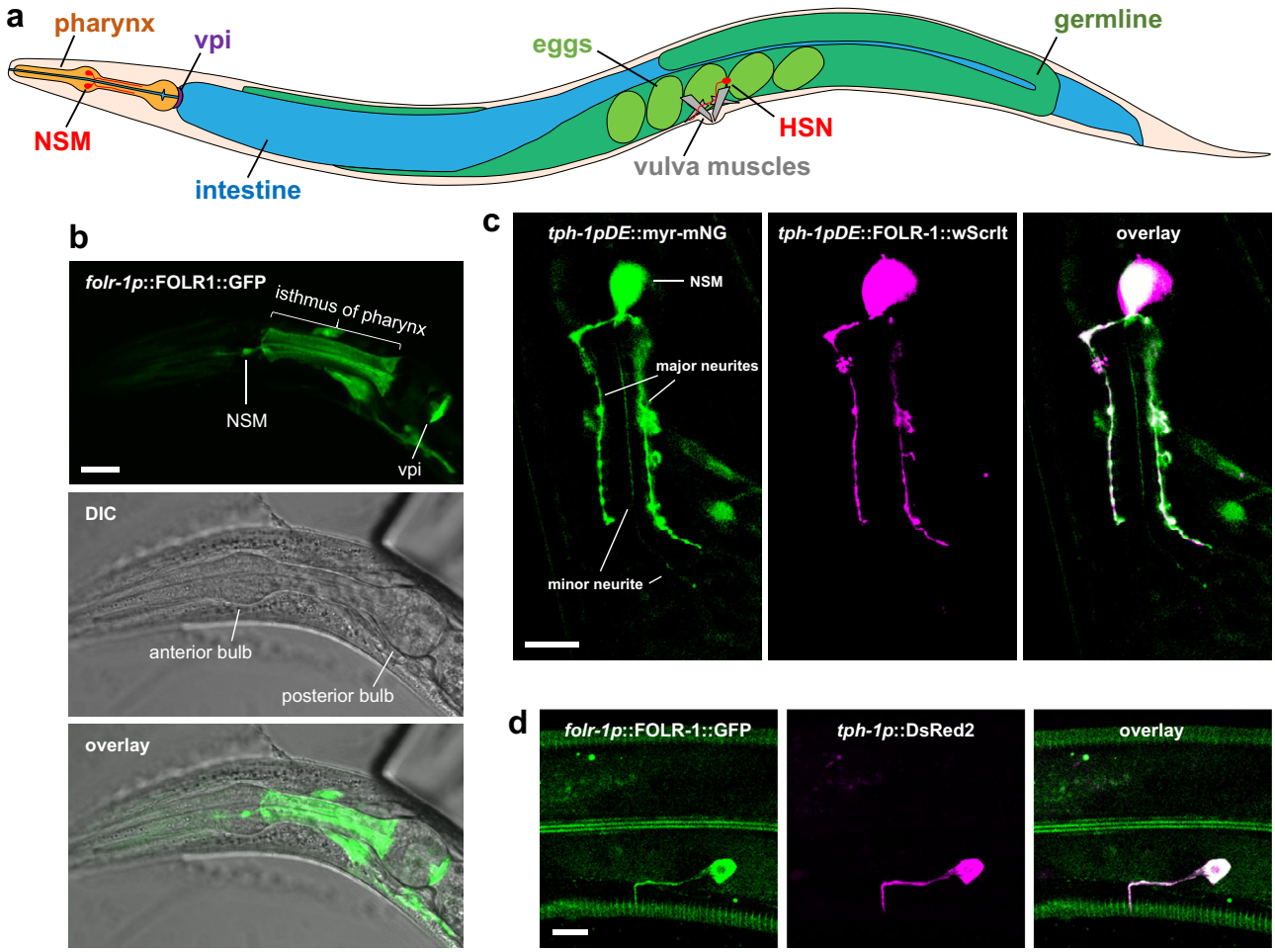

Fig. 1 | FOLR-1 localizes to NSM and HSN neurons. a Diagram of the *C. elegans* body plan showing the location of labeled tissues. Note that the HSN neuron is on the lateral surface, and only one HSN neuron is shown (the other is on the other lateral surface behind the intestine and germline). The extension of the HSN axon to the nerve ring between the two pharyngeal bulbs is not shown. **b** DIC and overlaid confocal maximum projection of *z*-sections for FOLR-1::GFP expressed using the *folr-1* promoter. Similar localization was observed in $n = 27$ animals from $n = 3$ independent experiments. **c** Confocal maximum projection of *z*-sections of FOLR-1::wrmScarlet and myristoylated mNeonGreen, which highlights the plasma membrane; with both expressed using the NSM-specific promoter *tph-1pDE*. Similar localization was observed in $n = 35$ animals from $n = 4$ independent experiments. **d** Confocal maximum projection of *z*-sections of FOLR-1::GFP expressed using the *folr-1* promoter and DsRed expressed in HSN neurons using the *tph-1* promoter. Similar localization was observed in $n = 24$ animals from $n = 4$ independent experiments. Scale bars are 10 μm. vpi pharyngeal-intestinal valve cells.

Egg laying is a complex behavior with multiple inputs[23]. Because of the day-to-day variability in egg-laying rate, we compared egg laying for animals with the experimental condition to animals with the control condition at the same time. Adult hermaphrodites with one row of non-overlapping eggs in their uterus were used for all experimental analyses. These are approximately one-day-old adults.

We observed that 10F-THF stimulates egg laying in wild-type adult hermaphrodites that were starved for 30 min, with significantly more eggs laid over one hour, including within the first 5 min (Fig. 2a). In contrast, starved *folr-1(ek44)* adult hermaphrodites did not lay increased numbers of eggs in response to 10F-THF, indicating that the response to 10F-THF depends on the presence of FOLR-1 (Fig. 2a).

To determine the specificity of different folates for increasing egg laying, we tested three other folates that function in one-carbon metabolism: 5-methyl-THF; 5-formyl-THF; and THF. These three folates did not alter egg-laying rates in wild-type hermaphrodites (Fig. 2c). This implies that the FOLR-1-dependent pathway is specific for 10F-THF relative to other cellular folates.

To determine if the FOLR-1 pathway regulating egg laying is independent of metabolism, we utilized the pteroate DHP, which cannot be utilized in one-carbon metabolism by animals[9]. DHP increased egg laying in starved wild-type hermaphrodites when applied at the same concentration as 10F-THF (Fig. 2b). Notably, DHP did not increase egg laying in starved *folr-1(ek44)* mutants (Fig. 2b). This indicates that the DHP-mediated increase in egg laying in wild-type animals occurs through a FOLR-1-dependent process (Fig. 2b). These results imply that the FOLR-1-dependent increase in egg laying is independent of metabolism, and instead suggest a signaling event. A signaling pathway is consistent with the rapid timing of the increase in egg-laying rate (within 5 min). In contrast, it would be unclear how altering the levels of specific amino acids and nucleotides through one-carbon metabolism could induce egg laying in such a rapid manner.

GON-2 is required for egg laying in response to 10F-THF

Because HSN activation involves the entry of calcium[13], this raised the possibility that FOLR-1 could regulate calcium entry through interaction with a calcium channel. We considered the GON-2 TRPM calcium channel as a candidate interactor because FOLR-1 functions to increase the rate of germ cell proliferation[8], and GON-2 was previously identified as being important for germline development. At the non-permissive temperature, *gon-2(q388ts)* temperature-sensitive mutants exhibit a failure in the proliferation of the progenitor cells that form

https://doi.org/10.1038/s41467-024-52738-z

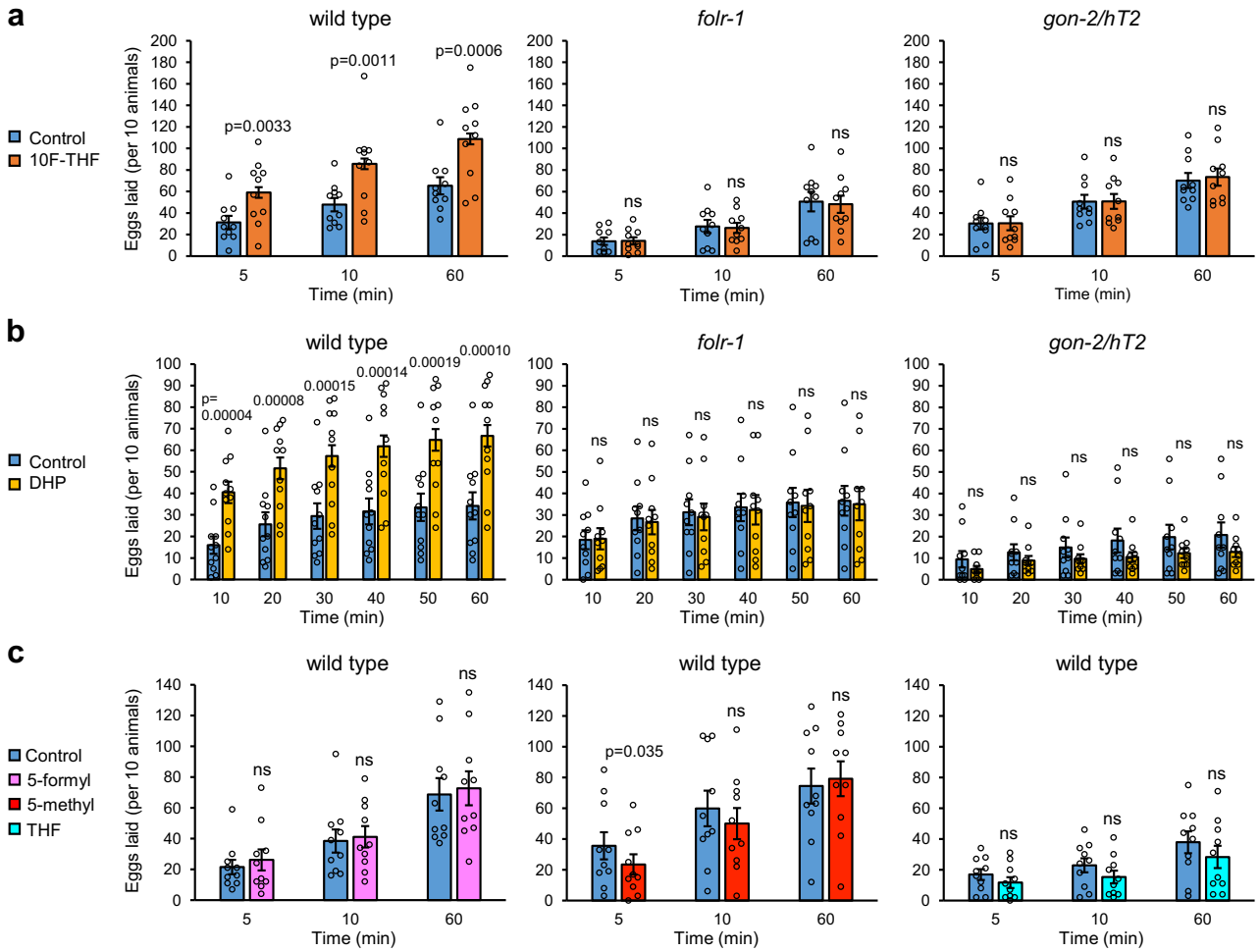

Fig. 2 | 10F-THF and DHP increase the rate of egg laying. a The average number of eggs laid in 5 min, 10 min, and 60 min for wild-type, *folr-1(ek44)*, and *gon-2(ok465)/hT2* adult hermaphrodites in response to 10F-THF or control buffer ($n = 10$). **b** The average number of eggs laid in 10 min intervals for wild-type, *folr-1(ek44)*, and *gon-2(ok465)/hT2* adult hermaphrodites in response to DHP or control buffer ($n = 11$, 10, and 10, respectively). **c** The average number of eggs laid by wild-type adult hermaphrodites in response to 5-formyl-THF, 5-methyl-THF, and THF ($n = 10$). Data are presented as mean ± SEM. A paired two-tailed Student's *t*-test was conducted for statistical analyses. For all figures, *p*-values that are significant ($p < 0.05$) are presented as exact values above the experimental condition and are relative to the corresponding control condition. The *p*-values that are not significant are denoted ns, *n* = groups of 10 animals. Source data are provided as a Source Data file.

the somatic gonad[24]. This leads to a failure to elongate the gonad and, therefore, a failure of germ cells within the gonad to divide (Supplementary Fig. 7). However, this failure of the somatic gonad precursors to divide is not observed in the *gon-2(ok465)* null allele, which deletes 507 base pairs, including the sixth transmembrane spanning segment, and is therefore expected to lack channel activity[25]. In homozygous *gon-2(ok465)* hermaphrodites, the somatic gonad precursors divide to form a normal-shaped somatic gonad, but there are fewer germ cells within the gonad (Supplementary Fig. 7). The *gon-2* null mutant phenotype suggests that GON-2 is required for germ cell proliferation independently of its role in generating the somatic gonad structure.

To determine if GON-2 is expressed in the HSN and NSM serotonergic neurons, we analyzed the expression of a GON-2::GFP transgene expressed from the *gon-2* promoter (the kind gift of Eric Lambie). *gon-2p*::GON-2::GFP expression is observed in both the HSN and NSM neurons (Fig. 3a, b). In the NSM neurons, *gon-2p*::GON-2::GFP localizes to the two larger neurites, similar to the FOLR-1 localization (Fig. 3b). To assess the effect of loss of GON-2 on the rate of egg laying, we utilized *gon-2(ok465)/hT2* heterozygotes, which appear superficially wild-type and generate eggs, unlike the sterile *gon-2(ok465)* homozygotes. Significantly, *gon-2(ok465)/hT2* heterozygotes did not exhibit increased egg laying in response to 10F-THF or DHP, indicating that GON-2 is also required for the response to folate/pteroate (Fig. 2a, b).

GON-2 can physically interact with FOLR-1

The expression of GON-2 in the same neurons and the similar abrogation of 10F-THF-induced egg laying suggests that GON-2 may function in the same pathway as FOLR-1. To test if GON-2 and FOLR-1 can physically interact, we expressed 3xHA epitope-tagged FOLR-1 and 3xFLAG epitope-tagged GON-2 in HEK293T cells. As negative controls, we utilized 3xHA-tagged ICAM1[26] and 3xFLAG-tagged FBXW7 (the kind gift of J. Swanger). GON-2::3xFLAG and FOLR-1::3xHA interacted with each other at significantly higher levels than with the negative control proteins (Fig. 3c, d). This suggests that the two proteins could promote egg laying through a shared pathway that involves their physical interaction.

FOLR-1 and GON-2 are required for 10F-THF activation of HSN

The HSN neuron has transient increases of cytosolic Ca^{2+} in the postsynaptic terminus that are coincident with egg-laying events (either singly or in bursts) and also occur in the absence of egg-laying events[15]. An integrated GCaMP5 genetic calcium reporter that is expressed in

https://doi.org/10.1038/s41467-024-52738-z

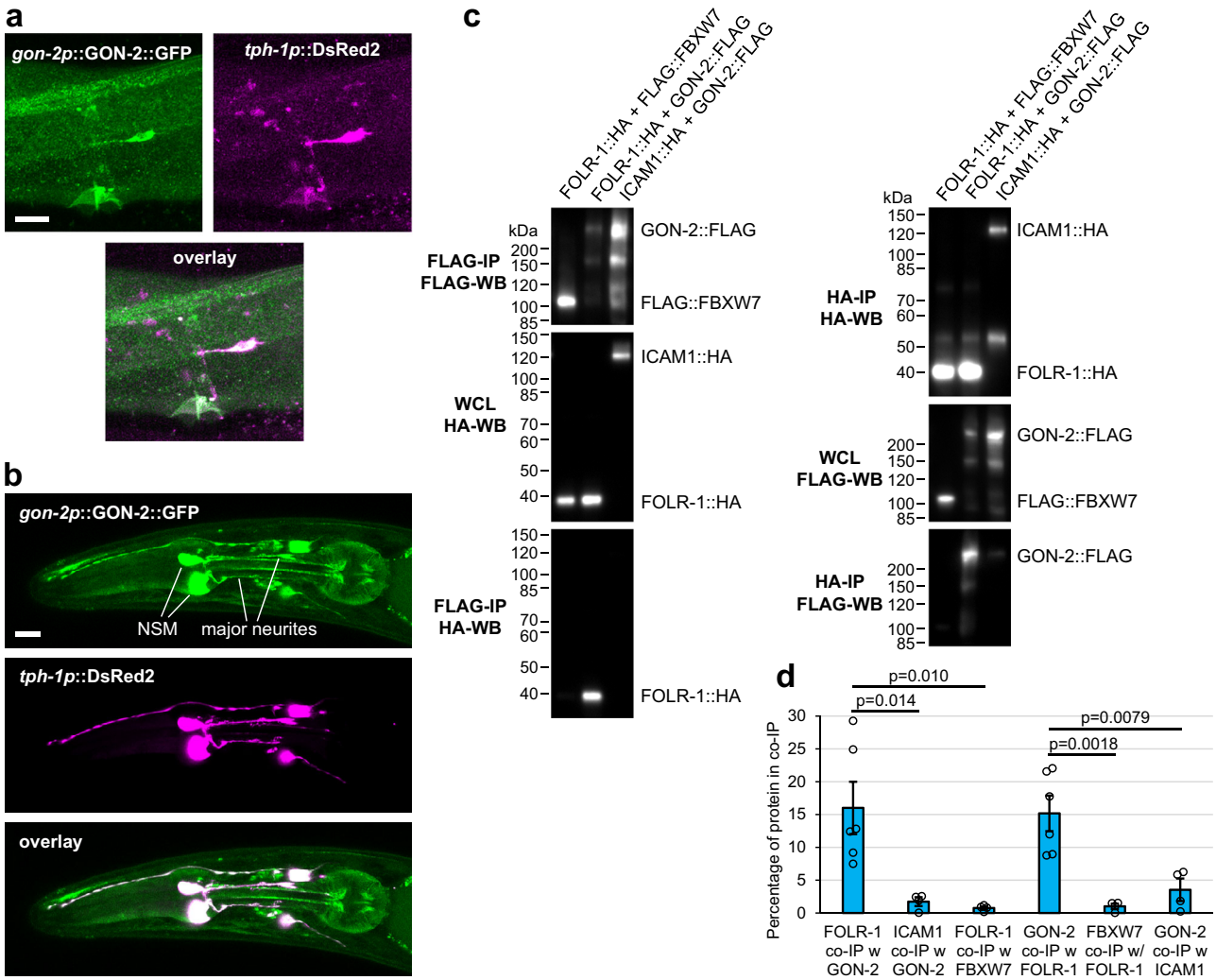

Fig. 3 | GON-2 is localized to HSN and NSM neurons and can physically associate with FOLR-1. a Overlaid confocal *z*-sections for GON-2::GFP expressed from its own promoter and DsRed expressed in HSN neurons using the *tph-1* promoter. Similar localization was observed in $n = 35$ animals from $n = 5$ independent experiments. **b** Confocal maximum projection of *z*-sections of GON-2::GFP expressed from its own promoter and DsRed expressed in the NSM neurons using the *tph-1* promoter. Similar localization was observed in $n = 19$ animals from $n = 3$ independent experiments. Scale bars are 10 μm. **c** Physical interaction of epitope-tagged FOLR-1::3xHA and GON-2::3xFLAG when expressed in HEK293T cells. Immunoprecipitation (IP) with anti-FLAG or anti-HA antibodies from HEK293T cells in which the labeled epitope-tagged proteins were co-expressed. Western blots (WB) of the whole cell lysate (WCL) or the IP were carried out with the antibodies listed. The first column shows the IP of 3xFLAG-tagged proteins (top panel), the expression of the 3xHA-tagged proteins in the WCL (middle panel), and the 3xHA-tagged proteins that physically associate with the immunoprecipitated 3xFLAG-tagged proteins (bottom panel). The second column shows the IP of 3xHA-tagged proteins (top panel), the expression of the 3xFLAG-tagged proteins in the WCL (middle panel), and the 3xFLAG-tagged proteins that physically associate with the immunoprecipitated 3xHA-tagged proteins (bottom panel). Similar results were obtained in at least four independent co-IP experiments, which are quantified in (**d**). **d** The percentage of expressed 3xFLAG- and 3xHA-tagged protein co-immunoprecipitated in co-IP experiments (from left to right, $n = 6, 4, 4, 6, 4$, and 4). Each *n* represents an independent co-IP experiment initiated with independent transfections of expression constructs into distinct cell populations. Asterisks above the lines signify statistical comparisons below the ends of the lines. Data are presented as mean ± SEM (**d**). Unpaired two-tailed Student's *t*-test was conducted for statistical analysis (**d**). Source data are provided as a Source Data file. Scale bars are 10 μm. WCL whole cell lysate, IP immunoprecipitation, WB western blot, co-IP co-immunoprecipitation, w with.

HSN[15] allows visualization of Ca^{2+} transients. To assess the effect of 10F-THF on HSN transients, adult hermaphrodites were starved for 30 min in M9 buffer and then mounted on a slide in 5 μl of 10F-THF or control buffer. Wild-type hermaphrodites had significantly more HSN transients with 200 nM or 40 nM 10F-THF than buffer control (Fig. 4a, b). The increase in transients with 10F-THF was not observed for *folr-1(ek44)* or *gon-2(ok465)* mutant heterozygotes (Fig. 4a, b). We analyzed *gon-2* heterozygotes rather than *gon-2* homozygotes because the homozygotes do not produce eggs, and the presence of eggs is known to increase HSN transients[27].

Incubation with 200 nM DHP also produced more Ca^{2+} transients in wild-type animals than control buffer (Fig. 4c). Similar to treatment with 10F-THF, 200 nM DHP did not increase Ca^{2+} transients in *folr-1(ek44)* or *gon-2(ok465)* mutants (Fig. 4c). This implies that the FOLR-1 and GON-2-dependent HSN signaling is independent of metabolism. Incubation with the five-fold lower concentration of 40 nM DHP did not produce more Ca^{2+} transients in wild-type hermaphrodites (Fig. 4c). This suggests that 10F-THF is a more potent signaling molecule than DHP, as 10F-THF retains activity at 40 nM concentration. Notably, the physiological concentrations of 10F-THF or DHP that can activate HSN neurons are not known because the concentrations the animals are exposed to will presumably differ from the concentrations that cells are exposed to after ingestion of the folate/pteroate and dissemination to cells.

https://doi.org/10.1038/s41467-024-52738-z

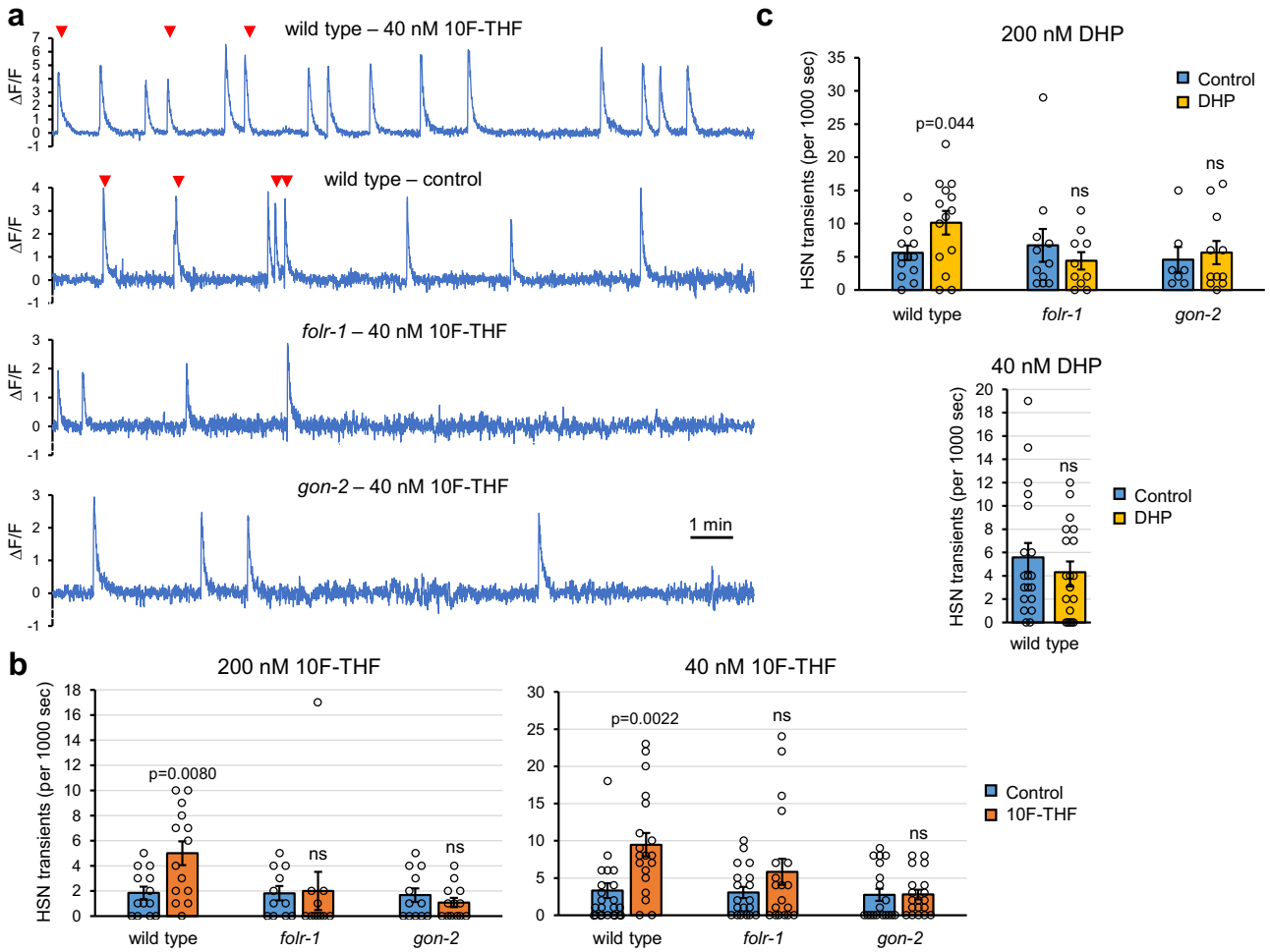

Fig. 4 | 10F-THF and DHP increase Ca^{2+} transients in HSN neurons. a Traces of fluorescence ($\Delta F/F$) for 1000 s from transgenic animals with GCaMP5 expressed in the HSN neurons for the indicated genotypes and treatment with 40 nM 10F-THF or control buffer. Egg-laying events are denoted with red arrowheads. **b** The number of Ca^{2+} transients in HSN neurons for the indicated genotypes and concentrations of 10F-THF or control buffer. *n* values for control and 200 nM 10F-THF, respectively, are: wild type (13, 14); *folr-1* (11, 11); *gon-2* (12, 13). The *n* = 19 for control and 40 nM 10F-THF for all genotypes. **c** The number of transients in HSN neurons for the indicated genotypes and concentrations of DHP or control buffer. The *n* values for control and 200 nM DHP, respectively, are: wild type (13, 14); *folr-1* (11, 10); *gon-2* (7, 11). *n* = 19 for control and 40 nM DHP for all genotypes. *n* = Movies of individual animals to assess Ca^{2+} transients (**b**, **c**). Data are presented as mean ± SEM. Unpaired two-tailed Student's *t*-tests were conducted for statistical analyses. Source data are provided as a Source Data file. ns not significant.

To determine if the serotonergic HSN neurons are important for the egg-laying response to 10F-THF, we utilized a gain-of-function mutation in the *egl-1* (egg-laying defective) BH3-only apoptotic regulator gene, *egl-1(n487)*. In *egl-1(n487)* mutants, HSN neurons are absent because they undergo apoptosis[28]. We observed that *egl-1(n487)* adult hermaphrodites do not have increased egg laying in response to 10F-THF (Fig. 5a). This implies that the HSN neurons are required for the response to 10F-THF.

To determine if serotonin is important for the egg-laying response, we analyzed *tph-1(mg280)* mutants, which are incapable of synthesizing serotonin[29]. *tph-1(mg280)* mutants do not have increased egg laying in response to 10F-THF (Fig. 5a). This suggests that the release of serotonin is required for the egg-laying response. We observed that both *tph-1(mg280)* and *egl-1(n487)* mutants laid less than one-quarter of the eggs of wild-type hermaphrodites at 60 min even in the absence of 10F-THF (Fig. 5a). This is expected, as both *egl-1(n487)* and *tph-1(mg280)* mutants are known to have reduced rates of egg laying[29,30].

FOLR-1 and GON-2 promote the activity of the NSM neurons

We wanted to determine in which tissues FOLR-1 expression was required for the HSN response to 10F-THF. Our strategy to assess the tissue(s) in which FOLR-1 impacts folate-stimulation of egg laying was to use the *folr-1(ek44)* mutant and express FOLR-1 in specific tissues. By comparing combinations of tissue expression of FOLR-1 with the egg-laying response to 10F-THF, the minimum tissue expression for FOLR-1 to rescue the egg-laying response to folate can be assessed.

We observed that the expression of FOLR-1 in both HSN and NSM (using the *egl-6*[31] and *tph-1DE*[21] promoters, respectively) did not rescue the egg-laying response to 10F-THF (Fig. 5b). This suggests that FOLR-1 is also needed in other tissues, potentially to bring 10F-THF into the body. A potential role for FOLR-1 in folate transport is anticipated by the observation that mammalian FOLR-1 mediates the transcytosis of folate across cell barriers[4–6]. We focused on the expression of FOLR-1 in the isthmus of the pharynx, which encases the NSM neurites and is in contact with the lumen of the digestive tract; and the pharyngeal-intestinal valve cells, which is in contact with the lumen of the digestive tract immediately after bacteria are disrupted in the posterior bulb of the pharynx (Fig. 1a).

We tested combinations of expression of FOLR-1 in HSN, NSM, the isthmus of the pharynx (using the *flr-4* promoter[32]), and the pharyngeal-intestinal valve cells (using the *cdf-1* promoter[33]). There are four combinations of three of the four tissues, and none of these combinations showed sustained, robust rescue (Fig. 5b). In contrast,

https://doi.org/10.1038/s41467-024-52738-z

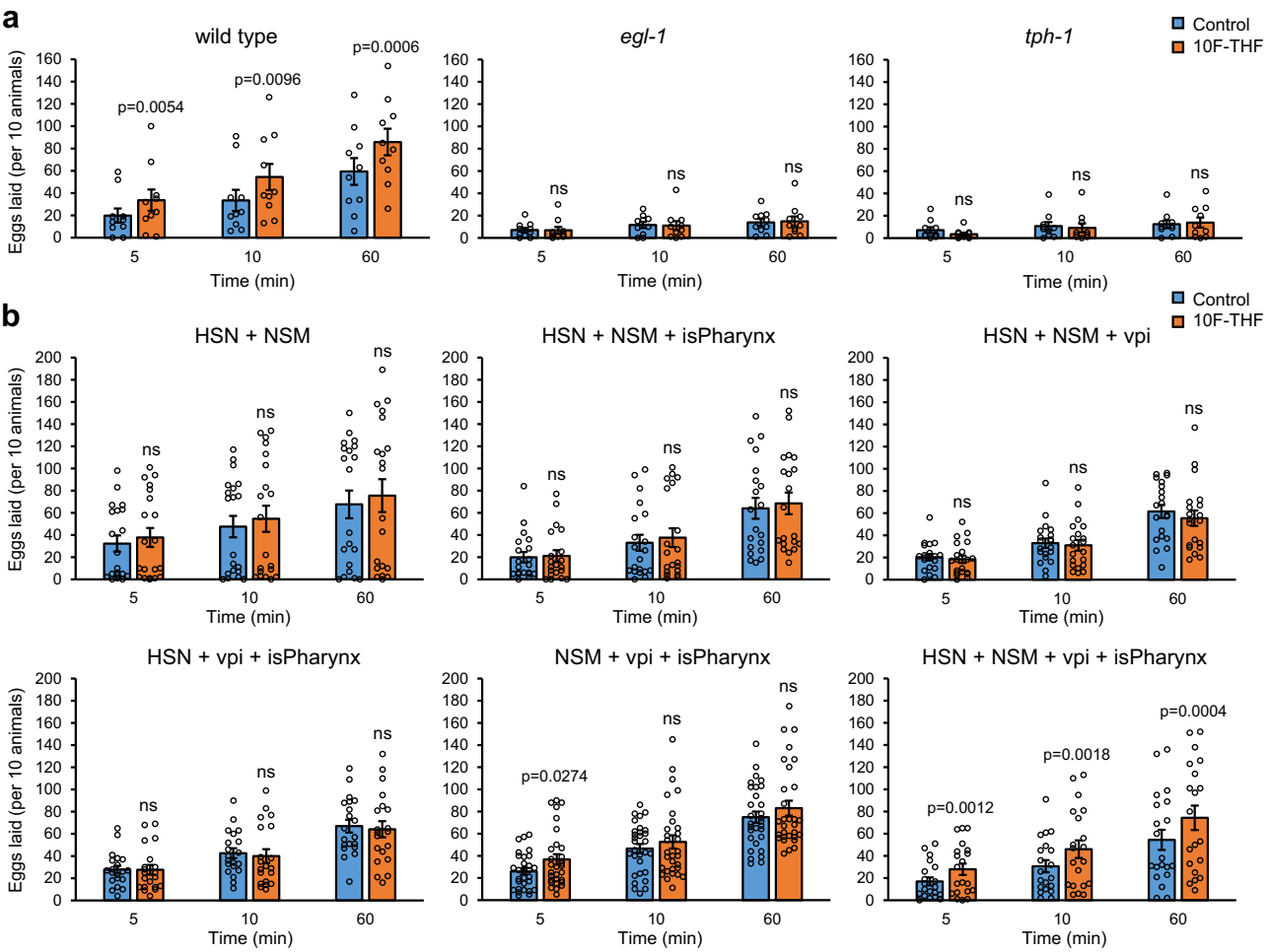

Fig. 5 | Tissue-specific expression of FOLR-1 to rescue *folr-1* mutants for egg laying in response to 10F-THF. a The number of eggs laid by wild type, *tph-1(mg280)* and *egl-1(n487)* mutants with 10F-THF or control buffer, added at the same concentration as for the experiments in Fig. 2 ($n = 10$). **b** The number of eggs laid by *folr-1(ek44)* mutant strains with FOLR-1 expressed in the indicated tissues in response to 10F-THF or control buffer ($n = 20$ except for NSM + vpi + isPharynx, which is $n = 30$). Data are presented as mean ± SEM. A paired two-tailed Student's *t*-test was conducted for statistical analyses, n = groups of ten animals. Source data are provided as a Source Data file. ns not significant, vpi pharyngeal-intestinal valve cells, isPharynx the isthmus of the pharynx.

expressing FOLR-1 in all four tissues rescued the folate stimulation of egg laying (Fig. 5b). This suggests that FOLR-1 expression is required in all four tissues to allow increased egg laying in response to 10F-THF. A model that fits these data is that FOLR-1 activity in the isthmus of the pharynx allows 10F-THF to reach the NSM neurites, and FOLR-1 activity in the pharyngeal-intestinal valve cells allows systemic release of 10F-THF into the body cavity where it can reach the HSN neurons.

We performed a similar rescue experiment to determine the tissues in which GON-2 must be expressed in *gon-2/hT2* heterozygotes in order to rescue egg laying in response to 10F-THF. We tested for rescue upon expressing GON-2 in NSM alone, HSN alone, and NSM and HSN. We observed rescue with expression in NSM alone and in NSM and HSN together, but not in HSN alone (Supplementary Fig. 8). The level of rescue was similar to what is observed when expressing GON-2 in NSM, HSN, the isthmus of the pharynx, and the pharyngeal-intestinal valve cells (Supplementary Fig. 8). Thus, it appears that expression of GON-2 in NSM is sufficient to rescue the egg-laying response to 10F-THF in *gon-2* heterozygotes. Because the rescue is in a heterozygous background, it is not possible to conclude that GON-2 is not needed in HSN, but rather that GON-2 expression beyond the heterozygous level in NSM is necessary for increased egg-laying in response to 10F-THF.

It has recently been observed that the NSM neurons take up serotonin released by HSN, and that this increases NSM effectiveness[34]. This indicates that serotonin can move between the two neurons, and that serotonin levels are rate-limiting for NSM activity. Feeding animals serotonin can functionally replace the loss of the HSN neurons, suggesting that systemic serotonin can impact egg laying[17]. It is likely that the systemic release of serotonin by NSM is taken up by HSN to increase its activity and/or affects the vulval muscles directly.

The observation that FOLR-1 and GON-2 expression in the NSM neurons contribute to egg laying suggested the possibility that 10F-THF could contribute to NSM activation. When starved animals ingest bacteria, NSM becomes activated resulting in a sustained increase in Ca^{2+} levels[13]. To assess the Ca^{2+} increase in the NSM neurons, we utilized transgenic strains expressing the genetic calcium reporter GCaMP7b[35] specifically in NSM (using the *tph-1pDE* promoter[21]). Starved wild-type, *folr-1*, and *gon-2* transgenic strains expressing GCaMP7b were allowed to encounter bacteria and the level of GCaMP7b epifluorescence was determined. We did not observe an obvious difference between wild-type, *folr-1*, and *gon-2* mutants in the $\Delta F/F$ GCaMP7b signal as the animals initially encountered bacteria (Supplementary Fig. 9a).

NSM activation results in the systemic release of serotonin, which stops the forward progress of starved animals[19]. We tested how quickly starved *folr-1* and *gon-2* mutant adults stopped when encountering bacteria. We observed that *gon-2* heterozygotes and *gon-2* homozygotes accelerated prior to reaching the bacteria relative to wild-type animals (Fig. 6a). Upon encountering bacteria, *gon-2* homozygotes, and to a lesser extent *gon-2/hT2* heterozygotes, had slower

https://doi.org/10.1038/s41467-024-52738-z

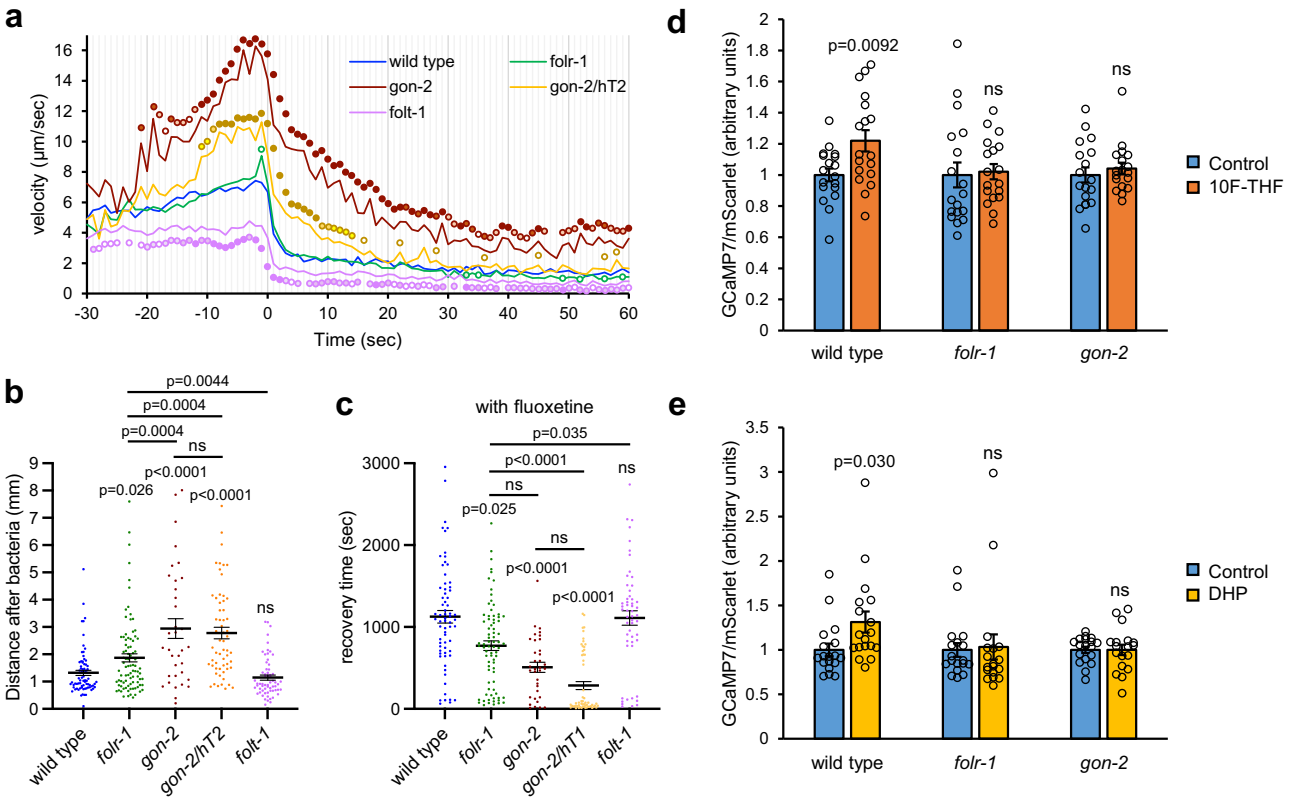

Fig. 6 | The effect of 10F-THF on NSM activity. a The average velocities of starved adult hermaphrodites as they approach and encounter bacteria (at time 0) for wild type, *folr-1(ek44)*, *gon-2(ok465)* homozygotes, *gon-2(ok465)/hT2* heterozygotes, and *folt-1(ok1460)*; $n = 105, 98, 32, 56, 71$, respectively. The *p*-values for individual data points are marked with color-coordinated circles. The *p*-value < 0.05 is denoted by a circle that has no fill; *p*-value < 0.01 light fill; *p*-value < 0.001 medium fill; and *p*-value < 0.0001 heavy fill. **b** The linear distance that starved adult hermaphrodites of the indicated genotypes travel in 2 min after encountering bacteria (from left to right, $n = 76, 87, 35, 59, 63$). **c** The recovery times for the indicated genotypes with fluoxetine pretreatment (from left to right, $n = 68, 77, 35, 58, 53$). n = Individual animals analyzed for movement (**a**–**c**). **d**, **e** The relative ratio of GCaMP7s/mScarlet expressed in NSM neurons for starved adult hermaphrodites exposed to 200 nM 10F-THF (**d**) or DHP (**e**) or control buffer for the genotypes indicated ($n = 18$ for **d**, **e**). n = Individual animals analyzed for GCaMP7s/mScarlet levels in NSM (**d**, **e**). Data are presented as mean ± SEM (**b**–**e**). Unpaired two-tailed Student's *t*-test (**a**, **d**, **e**), one-way ANOVA with Sidak Holm multiple comparisons (**b**), and Kruskal–Wallis test with Dunn's multiple comparisons (**c**) were used for statistical analyses. Source data are provided as a Source Data file. ns not significant.

deceleration than wild type (Fig. 6a). In contrast, *folr-1* mutants had only a minor increase in velocity prior to reaching the bacteria and a similar deceleration as wild type through the first minute after encountering bacteria.

To follow the strength of the NSM-mediated stoppage, we assessed the total movement of animals 2 min after encountering bacteria. We observed that *folr-1* mutants move ~41% greater distance than the wild type (Fig. 6b). *gon-2* homozygous and heterozygous mutants travel farther than *folr-1* mutants (Fig. 6b). Thus, GON-2 is more important for the NSM-mediated stopping behavior than FOLR-1, suggesting that GON-2 has contributions to this process that are independent of FOLR-1.

To determine if the absence of FOLR-1 or GON-2 alters the time for recovery from the NSM-mediated stoppage, we tested how quickly starved adults recover productive movement after encountering bacteria. In videos of starved animals encountering bacteria, a virtual circle of 2.5 mm diameter was placed around the point where each animal initially encountered bacteria. The time that the animals took to completely exit the circle was recorded as the recovery time. To potentiate the NSM-mediated stopping behavior, animals were pretreated with the serotonin-reuptake inhibitor fluoxetine, which increases the NSM-mediated stopping behavior[18]. Pre-treating animals with fluoxetine increased the recovery times for all genotypes, consistent with an increased perdurance of serotonin released from NSM (compare Supplementary Fig. 9b and Fig. 6c). The recovery time for *folr-1* mutants was 70% that of wild type in the absence of fluoxetine and 68.6% that of wild-type in the presence of fluoxetine (with the former not statistically significant, and the latter significant) (Fig. 6c, Supplementary Fig. 9b, and Supplementary Movie 1). *gon-2* homozygotes and *gon-2* heterozygotes had recovery times that were only 16% and 31% of the wild-type recovery time without fluoxetine, and 45% and 25% of the wild-type recovery time with fluoxetine, respectively (Fig. 6c, Supplementary Fig. 9b, and Supplementary Movies 2 and 3). These results suggest that FOLR-1 and GON-2 contribute to the perdurance of the NSM-stopping behavior. To determine if the reduced stopping behavior arose from a general lack of folate, we tested a mutant of the reduced folate carrier, *folt-1*, that has gross defects in folate transport[36]. *folt-1* mutants had recovery times and movement after encountering bacteria that were similar to that of the wild type (Fig. 6b, c, Supplementary Fig. 9b, and Supplementary Movie 4). That the gross defects in folate transport in the *folt-1* mutant did not engender shorter recovery times, suggests that the shorter recovery times observed for *folr-1* and *gon-2* mutants do not arise from a general loss of folate for metabolism.

To directly determine if the NSM neurons respond to 10F-THF, we utilized transgenic strains with GCaMP7s::P2A::mScarlet expressed in the NSM neurons. The inclusion of the P2A ribosome skipping sequence ensures that each mRNA transcript produces both GCaMP7s and mScarlet. This allows mScarlet to function as an expression control to allow ratiometric analysis of any increase in NSM GCaMP7s

signal as animals encounter 10F-THF. Transgenic strains with this reporter were placed in 200 nM 10F-THF or control buffer for 4 min and then GCaMP7s and mScarlet fluorescence intensities were quantified. The GCaMP7s-to-mScarlet ratio in a wild-type background increased 22% with 200 nM 10F-THF relative to the control buffer, which was significant ($p < 0.01$ level) (Fig. 6d). In contrast, *folr-1(ek44)* and *gon-2(ok465)* mutants did not have significant increases in the GCaMP7s-to-mScarlet signal relative to control buffer (Fig. 6d). The increase in the GCaMP7-to-mScarlet ratio in wild type is also observed in response to 200 nM DHP, with a statistically significant 31% increase (Fig. 6e). The GCaMP7s-to-mScarlet ratio was not statistically increased in *folr-1(ek44)* or *gon-2(ok465)* mutants in response to 200 nM DHP (Fig. 6e). Thus, NSM can be activated by both 10F-THF and DHP, albeit at a low level, in an FOLR-1- and GON-2-dependent manner that is independent of one-carbon metabolism.

Serotonin levels are not reduced in *folr-1* and *gon-2* mutants

Serotonin synthesis requires the pteridine tetrahydrobiopterin (BH4)[37]. Pteridines are related to folates and pteroates, as they contain pteridine rings. However, BH4 is not synthesized from a folate or pteroate precursor. Rather, BH4 is synthesized through a multistep process from GTP[37]. BH4 can be oxidized to become dihydrobiopterin (BH2), which does not function in serotonin synthesis. Dihydrofolate reductase (DHFR) can convert BH2 to BH4. In mammals, increases in folate can increase the expression of DHFR, which increases the level of BH4 via conversion from BH2[38,39]. It is not known if a similar linkage between folate levels and DHFR levels exists in *C. elegans*. Nevertheless, to determine if *folr-1* and *gon-2* mutants had a decrease in serotonin levels that might negatively impact NSM and HSN activity, we performed immunofluorescence with an anti-serotonin antibody. The level of serotonin in the NSM and HSN neurons were similar in *folr-1* mutants relative to wild type, but elevated in *gon-2* homozygotes and heterozygotes (Supplementary Fig. 10). Thus, the reduction in NSM- and HSN-regulated activities observed in *folr-1* and *gon-2* mutants is not due to a decrease in serotonin levels.

Discussion

We show that a specific folate, 10F-THF, can increase the rate of egg laying in *C. elegans*, while other cellular folates do not impact the rate of egg laying. FOLR-1 is required for the increased rate of egg laying in response to 10F-THF. The serotonergic HSN neuron, as well as the biosynthesis of serotonin, are also required for the egg-laying response to 10F-THF. Complementation rescue experiments show that FOLR-1 is required in four tissues for the egg-laying response to 10F-THF: the HSN and NSM serotonergic neurons, the pharyngeal-intestinal valve cells, and the isthmus of the pharynx. A plausible model is that FOLR-1 is required in the isthmus to transport 10F-THF to the NSM neurites, and in the pharyngeal-intestinal valve cells to transport 10F-THF to the body cavity. Presumably, the transport of folate through tissues by FOLR-1 in *C. elegans* would occur by a similar mechanism as the transcytosis of folates by mammalian FOLR1[4–6].

The presence of FOLR-1 allows 10F-THF to increase the number of Ca^{2+} transients in HSN neurons and modestly increase Ca^{2+} levels in NSM neurons. Notably, both the increase in egg laying and the increase in Ca^{2+} levels in NSM neurons occur within 5 min of the addition of 10F-THF. These short timeframes suggest that these processes are regulated by a signaling event rather than by changes in one-carbon metabolism that would alter the levels of nucleotides and amino acids. More direct evidence for a non-metabolic pathway is that the pteroate DHP, which cannot function in one-carbon metabolism in *C. elegans* or other animals[8–10], is also able to activate egg laying, increase Ca^{2+} transients in HSN neurons, and elevate Ca^{2+} levels in NSM neurons. All of these effects of DHP require the presence of FOLR-1, implying that FOLR-1 functions in a non-metabolic capacity to activate HSN and NSM.

We have shown that the GON-2 TRPM channel functions in the same neuronal processes as FOLR-1. GON-2, like FOLR-1, is expressed in both HSN and NSM neurons, and is required for the increased activity of these neurons in response to 10F-THF that translate into changes in behavior (increased egg laying and decreased motion, respectively). We provide evidence that FOLR-1 can physically interact with GON-2. This physical interaction suggests a mechanism through which FOLR-1 binding to folate modulates GON-2 activity to increase Ca^{2+} levels in NSM neurons and the rate of Ca^{2+} transients in HSN[40]. In *Drosophila* astrocytes, knockout of a TRPML Ca^{2+} channel reduces the number of Ca^{2+} transients but does not abolish them, providing a prior example of a TRPM channel whose activity increases the number of Ca^{2+} transients[41].

GON-2 is most closely related to the human TRPM7 channel, and both channels can transport Ca^{2+} and Mg^{2+} ions[42–44]. While the folate receptor has not previously been implicated in neuronal activation in any species, the closest homolog of GON-2 in vertebrates has known roles in promoting neuronal activity. In rat sympathetic neurons, TRPM7 increases the levels of acetylcholine neurotransmitter[45]. In mice, TRPM7 promotes neurite outgrowth of primary hippocampal neurons, with knockdown of TRPM7 reducing Ca^{2+} influx[46]. In zebrafish, TRPM7 is required for sensory neurons to conduct signals to the hindbrain[47].

Inactivation of *gon-2* in a heterozygous manner is sufficient to abrogate the increase in the rate of egg laying in response to folate. Other *egl* genes act as loss-of-function heterozygotes to reduce egg-laying rates, these include *egl-10* and *egl-30*[30,48,49]. This suggests that egg laying is often sensitive to the level of gene regulators. Notably, heterozygous mutation of *gon-2* also affects the NSM-mediated stopping behavior. The recovery times for NSM-mediated stopping are similar in *gon-2* heterozygotes and homozygotes, although the homozygotes are more resistant to the initial stopping behavior. The reason that the heterozygous *gon-2* mutation has effects that are almost as strong as the homozygous *gon-2* mutant is not known. One possibility is that GON-2 interaction with FOLR-1 only occurs when GON-2 is at sufficiently high concentrations.

Our study shows that the folate 10F-THF and the pteroate DHP are able to activate HSN and NSM neurons through a FOLR-1-dependent process. In contrast, other folates involved in one-carbon metabolism, such as 5-methyl-THF, 5-formyl-THF, and THF, do not activate these neurons. This specificity was also observed for 10F-THF and DHP stimulating the FOLR-1-dependent increase in germ cell proliferation[8]. 10F-THF and DHP do not share unique structural features compared to other folates (Supplementary Fig. 1). Therefore, we are unsure why 10F-THF and DHP would activate the FOLR-1-dependent process, while the other folates do not. There is, however, a functional argument for why 10F-THF and DHP could have been evolutionarily selected for this role in that both compounds are highly unstable relative to other folates[50] (see Schircks Laboratories Pteridine List, http://www.schircks.ch/pteridines/sys/pteridines_alphabetically_frame22.htm). Our results suggest that *C. elegans* utilizes 10F-THF and DHP as markers of ingested bacteria in order to regulate cellular and behavioral processes that are responsive to ingested bacteria. The use of unstable folate and pteroate allows a tighter linkage between the ingestion of bacteria and signaling. It also may allow *C. elegans* to distinguish the quality of different food sources. For example, the ingestion of healthy, live bacteria would provide 10F-THF and DHP, while these would presumably be missing from dead bacteria due to their instability.

Recently, another study showed that folate increases the number of Ca^{2+} transients in the neural plate cells of *Xenopus* embryos[51]. That study showed that knockdown of *FOLR1* reduces the number of spontaneous Ca^{2+} transients in neural plate cells. The study also showed that FOLR1 is required for neural tube formation in *Xenopus*. The addition of pteroate was able to rescue neural tube formation in FOLR1 knockdown embryos, suggesting that FOLR1 promotes neural tube closure independently of one-carbon metabolism[51]. In combination with our results, this suggests that the role of FOLR1 in mediating

signaling via calcium entry independently of metabolism is evolutionarily conserved from *C. elegans* to vertebrates.

In *C. elegans*, FOLR-1 is only expressed in a subset of neurons. If FOLR-1 were required for neuronal function in general, e.g., to provide folates for metabolism, then one would expect FOLR-1 to be more broadly expressed in neurons. Instead, the restricted expression of FOLR-1 in only a subset of neurons is more consistent with a role in regulating the activity of those neurons. A similar specificity of FOLR1 expression is observed in the developing mouse brain where FOLR1 is restricted to the mesencephalic floor plate, which gives rise to midbrain dopaminergic neurons[52]. The expression of FOLR1 in that context is so specific that affinity capture of FOLR1-expressing cells can be used to separate relatively pure populations of dopaminergic neurons from non-dopaminergic neurons and glial cells that do not express FOLR1[52]. Therefore, in both mice and *C. elegans*, FOLR1 has restricted expression in a subset of neurons, consistent with a role in signaling rather than providing folate for metabolism.

In *C. elegans*, FOLR-1 activates neurons that release serotonin to engender long-range effects. NSM releases serotonin in a systemic manner that causes body wall muscles to reduce their contractions, and, as our results suggest, increases the rate of egg laying. The release of serotonin by HSN, while locally affecting the vulval muscles, can impact the activity of NSM via the uptake of HSN-released serotonin by NSM[34] neurons, thereby demonstrating a similar long-range effect. Approximately half of the classes of neurons in *C. elegans* (52 of 118) express a serotonin receptor[53]. The release of serotonin by NSM is associated with changes in the activity of 45% of all neurons, reflecting a broad impact on neuronal activity[53]. Therefore, serotonin acts as a neuromodulator in *C. elegans* to alter the activity of other neurons in a long-range, systemic manner. Notably, in newborn mice, FOLR1 is enriched in the dopaminergic neurons of the ventral tegmental area region of the midbrain[54], which mediates the long-range release of dopamine into the prefrontal cortex[55]. This raises the intriguing possibility that the folate receptor may modulate neural activity in response to folates throughout diverse animal species.

Our observations are consistent with FOLR-1 functioning to modulate neural activity in response to a signal that marks a state change (from starvation to the availability of high-quality food). This is mediated by the release of serotonin, which can act as a neuromodulator to alter the activity of the large number of neurons that contain serotonin receptors[53], as well as affecting body-wall muscles to produce immediate behavioral changes. The expression of murine FOLR1 specifically in the dopaminergic neurons of the mouse midbrain suggests the possibility of a similar long-range alteration in neuron activity. It would be useful for future experiments to assess the role of the folate receptor in neuromodulation in other animals to determine if this role is broadly conserved.

Methods

C. elegans culture

C. elegans strains were maintained at 20 °C on the conventional diet of *Escherichia coli* strain OP50 bacteria according to standard protocols[56]. *C. elegans* strains are listed in Supplementary Table 1.

Adult hermaphrodites with one row of eggs were used for many experiments. These animals were obtained from cultures where the leading edge of progeny was one-day-old adults. To obtain these cultures, 8–12 L4-stage larvae were placed on 10 cm NGM agar plates[56] seeded with OP50 bacteria. After three days, the leading edge of the progeny were one-day-old adults, and those with one row of eggs were selected.

Generating the *folr-1(ek44)* mutation

We used CRISPR/Cas9-mediated mutagenesis to generate the *folr-1(ek44)* mutation. Recombinant Cas9 enzyme with an N-terminal HIS6 epitope-tag sequence was purified for use in the experiment. The pHO4d-Cas9 plasmid[57], which expresses HIS6-Cas9, was introduced into BL21(DE3)pLysS bacteria. HIS6-Cas9 protein was purified from the induced bacteria using Ni-NTA resin (Qiagen) according to the manufacturer's instructions. The *folr-1* crRNA (Synthego) targets the second exon of *folr-1* and has the targeting sequence: GUAUAUGGAGAC ACAUGCCG. CRISPR/Cas9 was assembled in vitro according to Synthego instructions with 14.1 μM Cas9 and 14.1 μM annealed crRNA and tracrRNA (Synthego). 71% of the crRNA/tracrRNA targeted the N-terminus of the *folr-1* gene and 29% targeted the *dpy-10* gene (targeting sequence: GCUACCAUAGGCACCACGAG). A single-stranded oligodeoxynucleotide (ssODN) for *dpy-10* was included in the injection mix[58]: CACTTGAACTTCAATACGGCAAGATGAGAATGACTGGAAACC GTACCGCATGCGGTGCCTATGGTAGCGGAGCTTCACATGGCTTCAGA CCAACAGCCTA. The CRISPR/Cas9 targeting of the *dpy-10* gene produces Rol (roller) phenotypes when rescued by the *dpy-10* ssODN, and Dpy (dumpy) phenotypes when insertion/deletion mutations are homozygous. N2 Bristol wild-type animals were injected, and Dpy and Rol progeny were collected and screened for deletion mutations in the *folr-1* gene by PCR followed by running the PCR products on 15% acrylamide gels, as described[59]. The *folr-1(ek44)* mutation was made homozygous, and the deletion site was confirmed by sequencing.

Expression constructs

Subcloning was accomplished using the In-Fusion cloning kit, according to the manufacturer's instructions (Takara Bio USA, Inc.). Constructs for *folr-1* expression in *C. elegans* utilize genomic sequence. Constructs for *folr-1* or *gon-2* expression in mammalian cells utilize cDNA sequences.

The expression module *folr-1p*::FOLR-1::eGFP::*tbb-2* 3′ UTR was cloned into plasmid pCFJ350[60]. The expression module includes 1857 bp of *folr-1* regulatory sequence and the *folr-1* genomic coding sequence not including the stop codon; a linker encoding GTSRGGGSGGGSGGG amino acids; *a C. elegans* codon-optimized GFP that includes *smu-1* introns to facilitate germline expression[61]; and 291 bp of the *tbb-2* 3′ UTR.

The *tph-1pDE*::FOLR-1::wrmScarlet::*unc-54* 3′UTR expression module was placed in the plasmid pCFJ350. The *folr-1* genomic sequence encompassing the open reading frame without the STOP codon was used. The *tph-1DE* promoter sequence is a truncation that was modeled on the *tph-1DE* promoter that expresses specifically in NSM neurons[21]. The published *tph-1DE* promoter includes 158 base pairs before the ATG start codon, the coding section of exon 1 (86 bp), the first intron (374 bp), and the first 13 bp of exon 2[21]. Here the *tph-1DE* promoter was modified by substituting the first exon of *folr-1* for the first coding exon of *tph-1* and inserting the second *folr-1* exon in-frame directly after the first *tph-1* intron. The region before the first *tph-1* exon begins with the 5′ sequence CGTGCCGAATTCCAGAAGCACCA and ends with the 3′ sequence GTAGCATTGCTCTCTTCAATCAT. The first *tph-1* intron starts with the 5′ sequence GTAAGTTTTCATCTT TCAAATCT and ends with the 3′ sequence ATCAGTAATTTCT GTACTTTCAG. The *folr-1* sequence does not include a stop codon, and is followed by a 6 bp spacer (GCTAGC) and then the wrmScarlet coding sequence[62].

The *tph-1pDE*::myr-mNeonGreen::*unc-54* 3′UTR expression module was placed in the plasmid pCFJ350. The *tph-1DE* promoter is fused in-frame to *a C. elegans*-codon-optimized myristoylated-mNeonGreen[63]. The in-frame fusion includes the first exon and one bp of exon 2 of the *tph-1* gene. The *tph-1pDE*::GCaMP7b::*unc-54* 3′UTR, *tph-1pDE*::GCaMP7s::P2A::mScarlet::*unc-54* 3′UTR, and *tph-1pDE*::FOLR-1::*unc-54* 3′UTR expression modules were placed in the plasmid pCFJ350. The GCaMP7s::P2A::mScarlet module was the kind gift of Stephen A. Vella.

The *egl-6p*::FOLR-1::*unc-54* 3′UTR expression module, for HSN expression[64], was placed in the plasmid pCFJ350. The *egl-6* promoter encompasses 2556 bp that begins with the 5′ sequence TTTCTTGTCGTTTTGCTCACAAC and ends with the

3′ sequence TCCCATATTTGCTTCCCTATTCG, similar to that previously described[64]. The *flr-4p*::FOLR-1::*unc-54* 3′UTR expression module, for expression in the isthmus of the pharynx[32], was placed in the plasmid pCFJ350. The *flr-4* promoter encompasses 1376 bp that begins with the 5′ sequence TATTGCAGCATTTGATTTTGCAT and ends just prior to the *flr-4* start ATG with the 3′ sequence TGTCGAGTTT GGAGCCCACGGGA. The *cdf-1p*::FOLR-1::*unc-54* 3′UTR expression module, for expression in the pharyngeal-intestinal valve cells[65], was placed in the plasmid pCFJ350. The *cdf-1* promoter includes 1548 bp that begins with the 5′ sequence CCGTTGTTGAGAGCT and ends with the 3′ sequence GGTTTGTCATCAACTGGAACAAAAAAAAAC.

To express FOLR-1 in human HEK293T cells, the *folr-1* open reading frame (ORF) was synthesized with humanized codons and a C-terminal 3xHA epitope tag (Biomatik) and placed in the pcDNA3.1(−) expression vector (Thermo Fisher Scientific). To express GON-2 in HEK293T cells (ATCC catalog number CRL-3216), the *gon-2* ORF was synthesized in three pieces with humanized codons and a C-terminal 3xFLAG tag (Biomatik). Restriction digestion and ligation were used to create one contiguous *gon-2*::3xFLAG ORF in pcDNA3.1(−). The control plasmid pCAG CAG Glucagon-ICAM1-3xHA-pre-mGRASP[26] was obtained from AddGene (the kind gift of Alice Ting). The control plasmid pFLAG-FBW7α was the kind gift of Jherek Swanger.

Rescue constructs for GON-2 were created with the same promoter regions as for the FOLR-1 rescue constructs (above) and in the same pCFJ350 vector. Due to the large size of the genomic *gon-2* gene (22.5 kb), which makes cloning genomic DNA difficult, the *gon-2* expression sequence includes the first 210 bp of *C. elegans gon-2* coding sequence with the remainder coming from the *gon-2* ORF sequence from the human expression construct described above. The first 210 bp of *gon-2* genomic DNA includes the first two exons and introns and part of the third exon in all constructs except for the *tph-1pDE* promoter expression module for which the first intron is from the *tph-1* gene.

Generation of transgenic strains

Transgenic strains containing extrachromosomal arrays were created by injection of uncut plasmid DNA into adult hermaphrodites using a Zeiss Jena injection apparatus with a Zeiss Axiovert 100 microscope. Injection needles (World Precision Instruments, 18120F-6) were pulled using a Sutter Instruments vertical needle puller. Injections of DNA into the germline of adult hermaphrodites were performed as described in ref. 66. pCFJ350/*folr-1p*::FOLR-1::GFP::*tbb-2* 3′UTR plasmid was injected into *unc-119(ed3)* mutant hermaphrodites at 100 ng/μl to create an extrachromosomal array. The pCFJ350 plasmid has *an unc-119(+)* gene and rescues the *unc-119(ed3)* Unc mutant phenotype.

Strains to rescue *folr-1(ek44)* mutants with modules that express FOLR-1 in selected tissues were injected as uncut plasmids into *folr-1(ek44) unc-119(ed3)* mutants at a concentration of 5 ng/μl for each expression plasmid with a total concentration of 100 ng/μl, with the difference made up with empty pCFJ350 vector. Two independent strains were tested for each rescue combination. The two strains gave similar results, and the data was combined.

Strains to rescue *gon-2(ok465)* mutants with modules that express GON-2 in selected tissues were injected as uncut plasmids into *gon-2(ok465)/hT2 unc-119(ed3)* mutants at a concentration of 25 ng/ul for each expression plasmid.

A single genomic insertion of the *tph-1p*::GCaMP7s::P2A::mScarlet::*unc54* 3′UTR reporter was created using the MosSCI Mos1 transposon targeting system[67], placing the transgene in the *ttTi5605* MosSCI site on chromosome II. An extrachromosomal array with the pCFJ350/*tph-1p*::GCaMP7b::*unc54* 3′UTR plasmid, injected uncut at 100 ng/μl into *unc-119(ed3)* mutant hermaphrodites, was integrated into the genome after irradiation with 4000 rad from a C-60 irradiator (located at the University of Georgia Center for Applied Isotope Studies).

Folates

The following folates and pteroates were used: 5-formyl-5,6,7,8-tetrahydrofolic acid (5-formyl-THF) (Sigma); (6S)−5-methyl-5,6,7,8-tetrahydrofolic acid (5-methyl-THF) (Schircks Laboratories); 5,6,7,8-tetrahydrofolic acid (THF) (Merck); and 7,8-dihydropteroate (DHP) (Schircks Laboratories). The 5,10-methenyl-5,6,7,8-tetrahydrofolic acid (5,10-methenyl-THF) was synthesized from 5-formyl-THF as described[68]. Briefly, 5-formyl-THF was brought to pH 1.5 with HCl and left at 4 °C for 24 h. The conversion is quantitative[68], and was checked by absorbance spectroscopy. The conversion of 5,10-methenyl-THF to 10-formyl-5,6,7,8-tetrahydrofolic acid (10-formyl-THF) was as described[68], with the details in the next section. Absorbance spectra showing the conversion of 5,10-methenyl-THF to 10F-THF are presented in Supplementary Fig. 11.

Egg-laying assay

Adult hermaphrodites with a single row of eggs in their uterus were used for the egg-laying assay. The hermaphrodites were placed in the center of unseeded 6 cm NGM agar plates. Approximately 25 hermaphrodites that left the center region of the NGM plate (and were not in contact with bacteria) were picked (using a flat platinum wire pick) into a drop of 200 μl M9 buffer[56] on an unseeded 6 cm or 10 cm M9-agarose plate (made with M9 buffer and 1.5% agarose (A9539, Sigma Aldrich)). This wash removed any residual bacteria. The animals were then transferred to a second 200 μl drop of M9 buffer and incubated for 30 min. At the end of the 30 min, plates were prepared with folate, pteroate, or buffer control. Ten micromolar 10F-THF was freshly created by adding 1.2 μl of 500 μM 5,10-methenyl-THF to 58.8 μl of 50 mM Tris (pH 8.5). The higher pH stoichiometrically converts 5,10-methenyl-THF to 10F-THF[68]. After incubation for 4 min, 25 μl of the 10 μM 10F-THF was spread onto a 6 cm M9-agarose plate. Control plates were created the same way except sterile water (SH30538.03, Hyclone) was substituted for the 1.2 μl of 500 μM 5,10-methenyl-THF. Other folates and pteroates (which did not require conversion) were diluted into PBS (SH30256.01, Hyclone) to a final concentration of 10 μM, and 25 μl was spread onto a 6 cm M9-agarose plate. For these folates, PBS was used as the control solution.

Ten starved (M9-washed) worms were placed (using a flat platinum wire pick) in a 10 μl drop of M9 buffer on plates spread with 10F-THF or control buffer. Swimming worms in the 10 μl M9 drop laid very few eggs. Time zero was set to when the M9 drop was completely absorbed into the plate, and the animals were able to move with sinusoidal motions. Animals were observed with a Zeiss Stemi SV 6 stereomicroscope. Eggs were counted at intervals of either every 10 min through 60 min, or at 5 min, 10 min, and 60 min intervals. At least ten replicates were carried out for each genotype/condition. M9 buffer and NGM agar were prepared as described[69].

Analysis of diffusion on plate surface for egg-laying assay

The concentration of folate on the surface of 6 cm M9-agarose plates after spreading 25 μl of 10 μM folate on the plate was estimated by observing the diffusion of bromophenol blue dye. Bromophenol blue has a molecular weight (670 Da) that is similar to that of 10F-THF (473 Da). Twenty-five microlitres of a saturated solution of bromophenol blue was spread on the surface of a 6 cm M9-agarose plate. It takes approximately 10 min from the time folate is spread on the plate to the drying of the M9 buffer with animals on the plate (the 0-time point). At 10 min post spreading (equivalent to the 0 time point) a 2 mm thin slice of the agarose was laid on its side on a microscope slide and imaged at 2400 dpi with a flatbed scanner (Epson 4870 Photo) using transillumination. Images were also made at 20 min and 70 min (equivalent to the 10 min and 60 min time points). Slices from three separate spread plates were imaged. The extent of diffusion was determined using Fiji software (Image J version 2.1.0/1.53s with plugins). The Plot Profile feature of Fiji was used to obtain the intensity at

each pixel of a vertical line from the top of the slice to the bottom (with two vertical lines analyzed per slice of M9-agarose). The background level was subtracted and the extent of diffusion in mm was determined for each vertical line. The average intensity for the area of diffusion was determined. The total volume of diffusion was determined by multiplying the area of the plate surface in mm^2 by the distance of diffusion into the plate in mm (to give the total volume of diffusion in μl, i.e., mm^3). The concentration on the surface of the plate was obtained by multiplying 10 μM (the initial concentration that was spread) by the ratio of the total dilution volume (i.e., 25 μl divided by the total volume of diffusion) and then multiplied by the ratio of the intensity of bromophenol blue at the surface relative to the average intensity in the total area of diffusion. The concentration at the surface was determined for each of the two vertical lines for each of the three cut slices, and averaged.

Analysis of HSN Ca^{2+} transients

Adult hermaphrodites with one row of eggs were starved in an M9 buffer as for egg-laying assays (described above). At the end of the 30-min starvation period, animals were mounted on a 2% agarose pad on a microscope slide (Globe Scientific, 1324W) with a 22 × 22 mm coverslip (VWR). Animals were imaged on a Zeiss Axioskop microscope. Images with 4 × 4 binning (512 × 512 pixels) were taken at four frames per second (fps) for 6000 frames using a Tucsen Dhyana 400 BSI V2 sCMOS camera in CMS mode that was controlled with Micromanager software (version 1.4.23). The first 2000 frames were not used because the initial pressure on the animal from adding the coverslip induced egg laying and HSN activity. This was consistent with the observation that internal pressure induces egg laying and HSN activity[27]. Some animals had excessive numbers of transients that suggested a defibrillation-like state that was operationally defined as 13 or more transients in 1000 frames (250 s). Animals with defibrillation-like transients were a small percentage of all genotypes and conditions, and were not included in the analysis. For quantitation, the mean value of the HSN signal in a 13 × 13-pixel circle was recorded for each frame using Fiji software. Background levels within the animal were obtained from a region with a low signal near the HSN, and the mean values in a 13 × 13-pixel circle were measured for 100 frames and averaged. The average background level was subtracted from each mean HSN signal to produce the mean-minus-background signal. If any HSN signal values were negative after subtracting the average background level, then the lowest mean HSN signal value was used as the background signal. Mean-minus-background signals for video frames that did not contain transients were averaged to produce the F value. $\Delta F/F$ was calculated as: (Mean − background signal minus F)/F.

GCaMP7s/mScarlet ratio

Transgenic strains that express *tph-1pDE*::GCaMP7s::P2A::mScarlet in the NSM neurons were analyzed. 60 adult hermaphrodites with one row of eggs were washed two times in 200 μl M9 buffer (as above) and incubated in a third drop of 200 μl M9 buffer to starve the animals. The hermaphrodites were analyzed after 1–4 h of starvation. For each data collection, three animals were placed on a 2% agarose pad (made with water) on a microscope slide (Globe Scientific) in 5 μl of either 200 nM 10F-THF (created freshly from 5,10-methenyl-THF and diluted in 2% sodium ascorbate to 200 nM) or 200 nM DHP in 2% sodium ascorbate, or matched buffer. Sodium ascorbate inhibits the oxidation of the reduced folate and pteroates. The animals were kept on the slide in the solution for 4 min and then a 22 × 22 mm no. 1 coverslip was gently applied. Animals were imaged with a 20× objective on a Zeiss Axioskop microscope. A Tucsen Dhyana 400 BSI V2 sCMOS camera was used to capture 1028 × 1028 pixel images at 1 fps for several seconds. The same exposure was used for all animals. Stimulatory folate/DHP and control sets of animals were alternately imaged. Images were analyzed using Fiji software. The strongest in-focus mean signal of the NSM neuron for GCaMP7s or mScarlet was obtained within a circle that is equivalent to a diameter of 6.5 μm on the slide. The mean background signal was obtained from the head region with the lowest signal using a circle of the same diameter. The mean background signal was subtracted from the GCaMP7s and mScarlet signals prior to calculating the GCaMP7s/mScarlet ratio.

Velocity and recovery time measurements

Adult hermaphrodites with one row of eggs (or equivalently sized *gon-2(ok465)* homozygotes that do not have eggs) were washed in three 200 μl drops of M9 buffer (as above) and then placed in 10 μl of M9 buffer on a 6 cm M9-agarose plate with or without 75 μg/ml fluoxetine. Once the 10 μl drop was absorbed into the plate (~15 min), the hermaphrodites were incubated on the plate for 30 min. A 6 cm NGM plate with a small circle of OP50 bacteria in the center was created by placing a 0.7–1.0 cm drop of saturated OP50 bacteria in LB medium on the plate and incubating overnight at room temperature. Between 8 and 18 animals were placed individually in 5 μl drops of M9 buffer located between the bacterial circle and the edge of the plate. The M9 liquid was absorbed into the plate, and the animals were imaged as they encountered the bacteria. Videos were captured on a Leica MZ10F stereomicroscope at 1 fps, using a Tucsen Dhyana BSI V2 sCMOS camera controlled by Micromanager software.

The velocity of animals was measured using the Manual Tracking plug-in available in Fiji software. The position of the tip of the tail was tracked in each frame. The time for recovery from stoppage was determined by placing a virtual circle on the video frames (equivalent to a diameter of 2.5 mm on the plate) centered on the point where the animal first encountered the bacteria. The number of seconds until the tip of the animal's tail left the circle was recorded as the recovery time. The linear distance moved was measured using the straight-line tool (Fiji software) to track the distance that the head of the animal moved after 2 min post-encountering bacteria.

Co-immunoprecipitation (co-IP) and western blotting

Human HEK293T cells were transiently transfected with plasmids expressing combinations of 3xHA- and 3xFLAG-epitope tagged proteins: FOLR-1::3xHA; GON-2::3xFLAG; ICAM1-3xHA; and 3xFLAG-FBXW7. DNA transfections used lipofectamine 3000 (Thermo Fisher Scientific) according to the manufacturer's instructions. Cells were harvested three days after transfection and lysed with IP lysis buffer (150 mM NaCl, 50 mM Tris (pH 8), 0.33% Triton X-100, 1.25× complete EDTA-free protease inhibitor (Roche)). Lysate was spun down at 21,000xg for 30 min at 4 °C. Part of the soluble lysate was kept as whole cell lysate (WCL). The remainder was split in half for immunoprecipitations (IPs) with added anti-FLAG M2 Affinity Gel (Sigma-Aldrich, A2220, lot number SLCG5835) or anti-HA Affinity Gel (Sigma-Aldrich, E6779, lot number SLCF6754); both at 5 μl of packed gel per 500 μl of lysate. The affinity gels were pre-blocked prior to use to reduce non-specific binding. Pre-blocking was carried out by incubating the affinity gels with 1.5% milk protein in IP buffer overnight at 4 °C. A stock solution of milk protein was created from 20% non-fat dry milk (Kroger) in IP lysis buffer, rotated for 30 min at 4 °C, centrifuged at 21,000xg for 25 min at 4 °C, and the soluble portion was used. The pre-blocked affinity gels were rotated in the cell lysate for 2 h at 4 °C. Beads were then spun out (500×*g* for 1 min) and washed five times with IP lysis buffer. Anti-HA affinity gels were boiled in SDS sample buffer. Anti-FLAG IPs were affinity eluted from the beads with 150 ng/μl 3xFLAG peptide (APExBIO) in IP lysis buffer for 20 min at room temperature. The affinity elution was repeated twice for 30 min and 20 min. The 3xFLAG peptide-eluted samples were combined and lysed in SDS sample buffer. For replicates of the co-IP experiment (Fig. 3d), anti-FLAG gels were boiled in SDS sample buffer, similar to the anti-HA affinity gels.

SDS-polyacrylamide gel electrophoresis was performed with 4–12% NuPAGE gels using MOPS buffer (Thermo Fisher Scientific). Proteins were transferred to the Immobilon-P PVDF membrane (Millipore). Membranes were stained with amido black, then blocked with blotto (5% non-fat dry milk protein in TBST (137 mM NaCl, 2.7 mM KCl, 15 mM Tris, 0.2% Tween-20)) for 30 min at room temperature. The primary antibodies used were mouse anti-FLAG (M2, Sigma-Aldrich, F3165) and rabbit anti-HA (71-5500, Thermo Fisher Scientific, lot XD345766), each at 1:20,000 dilution. Secondary antibodies were goat anti-mouse HRP (31432, Thermo Fisher Scientific) and goat anti-rabbit HRP (31462, Thermo Fisher Scientific), each at 1:20,000 dilution. Immunoblot bands were visualized with ECL Select Western Blotting Detection Reagent (Cytiva) using a ChemiDoc MP Imaging System (BioRad).

To determine the percentages of total protein that were co-precipitated, western blot bands were compared to the input WCL to produce a whole-cell-lysate equivalent (WCLE) value. Multiple dilutions of WCL were run, and the precipitated and co-precipitated bands were compared to WCL bands that were of higher and lower intensity. Linear regression was used to obtain the WCLE value for the precipitated and co-precipitated proteins. The percentage of total protein that co-precipitated was then calculated, taking into account the percentage of the primary protein that was precipitated. For example, if 70% of the total HA- protein was precipitated then the percentage of FLAG-protein that was co-precipitated with the HA-protein was calculated relative to 70% of the total FLAG protein in the lysate.

Microscopy

Non-confocal fluorescence and DIC images were obtained with a Zeiss Axioskop microscope, with images captured using Micromanager software (version 1.4.23) (Supplementary Figs. 2, 3, 7, and 10). Confocal images were taken on a Zeiss LSM 770 confocal (Fig. 1b), Zeiss LSM 880 confocal (Figs. 1d, 3a, and 3b), Zeiss ELYRA S1 (Supplementary Fig. 4), and Leica Thunder (Fig. 1c) microscopes. Confocal images for the Zeiss microscopes were captured with Zen Blue software (Zeiss). Images were processed with Adobe Photoshop (version 22.0.0) and Fiji software. Matched fluorescence images were processed identically and did not include gamma adjustments.

Anti-serotonin immunofluorescence

We followed a published anti-serotonin staining protocol[70]. In brief, young adult animals were fixed overnight in 4% paraformaldehyde in PBS, then washed with 0.5% Triton X-100 in PBS (TrPBS), then incubated overnight at 37 °C in 5% β-mercaptoethanol, 1% Triton X-100, 100 mM Tris (pH 7.4). Animals were washed in TrPBS, incubated in 2000 U/ml collagenase type IV (Sigma) in 1 mM $CaCl_2$, 1% Triton X-100, 100 mM Tris (pH 7.4), and then washed in TrPBS. Animals were blocked for 1 h with 1% BSA/TrPBS, and then incubated overnight with rabbit polyclonal anti-serotonin antibody (Neuromics Inc., high-titer anti-5HT, catalog number RA20080, lot number 403732) in 1% BSA/TrPBS. To remove background staining, the anti-serotonin antibody was precleared before use by incubation with worm acetone powder of the *tph-1(mg280)* mutant strain, prepared as described[71]. Briefly, mixed-stage *tph-1(mg280)* animals were grown on twenty 10 cm NGM plates and collected into 15 ml polystyrene tubes using water. The animals were cleaned using flotation on 30% sucrose[69], and then washed four times with water. Four parts of −20 °C acetone were added to one part of pelleted worms in a 15 ml polypropylene tube and then left on ice for 30 min with occasional vortexing. The fixed worms were spun down, and resuspended with 10 ml of −20 °C acetone, which was kept on ice for 10 min with occasional vortexing. The worms were washed once with −20 °C acetone, and then placed on aluminum foil to dry. The dried acetone-fixed worms were ground into a powder using a mortar and pestle. A 1:200 dilution of the anti-serotonin antibody was pre-incubated with 25 mg/ml acetone worm powder in 1% BSA/TrPBS for 2h at room temperature with rotation, and then the acetone worm powder was spun out at 21,000xg for 10 min. The precleared antibody was used for immunofluorescence without further dilution. Anti-rabbit IgG nano-antibody AlexaFluor 546 (ChromoTek Inc.) was used as the secondary antibody.

qRT-PCR

Total RNA was isolated from synchronized L4 stage wild type and *folr-1(ek44)* mutants using TRIzol reagent (Life Technologies) according to the manufacturer's instructions. RNA was reverse-transcribed into cDNA using the SuperScript IV First-Strand Synthesis System from Life Technologies, according to the manufacturer's instructions. The first-strand cDNA was used for PCR amplification of *folr-1* and the normalization control *rpl-19*, which encodes the large ribosomal subunit L-19. Reverse transcriptase polymerase chain reaction (RT-PCR) was performed using PowerUp SYBR Green Master Mix (Applied Biosystems) and analyzed using the CFX Connect Real-Time PCR Detection System (Bio-Rad). The primers used were: *folr-1*, forward: 5′-GAAGGAT GGTTTTGGACAAGTGTC-3′, reverse: 5′-GTAGCTAACCACTGGCTCA CG-3′; and *rpl-19*, forward: 5′-CGCGCAAAGGGAAACAACTT-3′, reverse: 5′-CTTGCGGCTCTCCTTGTTCT-3′. mRNA levels were normalized using *rpl-19* mRNA and the relative fold change was calculated using the ΔΔCt method. The normalized mRNA levels are reported in arbitrary units with the wild-type level set to 1.0.

Statistics and reproducibility

Egg-laying experiments with 10F-THF and DHP were performed at least two times with similar results. co-IP experiments were performed at least four times with similar results. Confocal, non-confocal fluorescence, and DIC microscopy imaging were performed at least three times with at least 19 animals imaged per condition, in all cases obtaining similar results. Analysis of HSN Ca^{2+} transients with 10F-THF was performed two times with similar results. Analyses of NSM Ca^{2+} levels in response to bacteria were performed two times with similar results. Analyses of animal velocities were performed two times with similar results. Anti-serotonin immunofluorescence experiments were performed two times with similar results. The statistical tests used are reported in the figure legends. Error bars reflect the standard error of the mean (SEM). Student's *t*-tests were two-sided and unpaired, except for egg-laying assays, which were paired. There is significant variation day-to-day in egg-laying rates due to the multiple inputs that can alter egg laying[23]. Because of the inherent variability in egg-laying rates, experimental folate/pteroate conditions were always paired to control samples prepared and assessed at the same time. The student's *t*-test was performed with Excel software (version 16.54). One-way ANOVA with Holm Sidak multiple comparisons was used for data with what appear to be normal distributions, but normality was not formally tested. The Kruskal–Wallis one-way ANOVA test with Dunn's multiple comparisons was used for data with clearly non-normal distributions. One-way ANOVA tests are *F*-tests, and were performed with Prism software (version 10.0.2). *n* Values reflect different animals or different groups of animals.

Reporting summary

Further information on research design is available in the Nature Portfolio Reporting Summary linked to this article.

Data availability

All data supporting the findings of this study are available within the paper and its supplementary information files. Biological material can be obtained from the corresponding author upon request. Source data are provided with this paper.

References

1. Ducker, G. S. & Rabinowitz, J. D. One-carbon metabolism in health and disease. *Cell Metab.* **25**, 27–42 (2017).

2. Petrova, B., Maynard, A. G., Wang, P. & Kanarek, N. Regulatory mechanisms of one-carbon metabolism enzymes. *J. Biol. Chem.* **299**, 105457 (2023).
3. Zhao, R., Diop-Bove, N., Visentin, M. & Goldman, I. D. Mechanisms of membrane transport of folates into cells and across epithelia. *Annu. Rev. Nutr.* **31**, 177–201 (2011).
4. Grapp, M. et al. Choroid plexus transcytosis and exosome shuttling deliver folate into brain parenchyma. *Nat. Commun.* **4**, 2123 (2013).
5. Henderson, G. I., Perez, T., Schenker, S., Mackins, J. & Antony, A. C. Maternal-to-fetal transfer of 5-methyltetrahydrofolate by the perfused human placental cotyledon: evidence for a concentrative role by placental folate receptors in fetal folate delivery. *J. Lab. Clin. Med.* **126**, 184–203 (1995).
6. Selhub, J., Emmanouel, D., Stavropoulos, T. & Arnold, R. Renal folate absorption and the kidney folate binding protein. I. Urinary clearance studies. *Am. J. Physiol.* **252**, F750–F756 (1987).
7. Nawaz, F. Z. & Kipreos, E. T. Emerging roles for folate receptor FOLR1 in signaling and cancer. *Trends Endocrinol. Metab.* **33**, 159–174 (2022).
8. Chaudhari, S. N. et al. Bacterial folates provide an exogenous signal for *C. elegans* germline stem cell proliferation. *Dev. Cell* **38**, 33–46 (2016).
9. Shane, B. Folate status assessment history: implications for measurement of biomarkers in NHANES. *Am. J. Clin. Nutr.* **94**, 337S–342S (2011).
10. Mathieu, M. et al. *Escherichia coli* FolC structure reveals an unexpected dihydrofolate binding site providing an attractive target for anti-microbial therapy. *J. Biol. Chem.* **280**, 18916–18922 (2005).
11. Leamon, C. P., You, F., Santhapuram, H. K., Fan, M. & Vlahov, I. R. Properties influencing the relative binding affinity of pteroate derivatives and drug conjugates thereof to the folate receptor. *Pharm. Res.* **26**, 1315–1323 (2009).
12. Taylor, S. R. et al. Molecular topography of an entire nervous system. *Cell* **184**, 4329–4347 e4323 (2021).
13. Iwanir, S. et al. Serotonin promotes exploitation in complex environments by accelerating decision-making. *BMC Biol.* **14**, 9 (2016).
14. Zhang, M. et al. A self-regulating feed-forward circuit controlling *C. elegans* egg-laying behavior. *Curr. Biol.* **18**, 1445–1455 (2008).
15. Collins, K. M. et al. Activity of the *C. elegans* egg-laying behavior circuit is controlled by competing activation and feedback inhibition. *Elife* **5**, e21126 (2016).
16. Horvitz, H. R., Chalfie, M., Trent, C., Sulston, J. E. & Evans, P. D. Serotonin and octopamine in the nematode *Caenorhabditis elegans*. *Science* **216**, 1012–1014 (1982).
17. Waggoner, L. E., Zhou, G. T., Schafer, R. W. & Schafer, W. R. Control of alternative behavioral states by serotonin in *Caenorhabditis elegans*. *Neuron* **21**, 203–214 (1998).
18. Sawin, E. R., Ranganathan, R. & Horvitz, H. R. *C. elegans* locomotory rate is modulated by the environment through a dopaminergic pathway and by experience through a serotonergic pathway. *Neuron* **26**, 619–631 (2000).
19. Gurel, G., Gustafson, M. A., Pepper, J. S., Horvitz, H. R. & Koelle, M. R. Receptors and other signaling proteins required for serotonin control of locomotion in *Caenorhabditis elegans*. *Genetics* **192**, 1359–1371 (2012).
20. Rhoades, J. L. et al. ASICs mediate food responses in an enteric serotonergic neuron that controls foraging behaviors. *Cell* **176**, 85–97 e14 (2019).
21. Sze, J. Y., Zhang, S., Li, J. & Ruvkun, G. The *C. elegans* POU-domain transcription factor UNC-86 regulates the *tph-1* tryptophan hydroxylase gene and neurite outgrowth in specific serotonergic neurons. *Development* **129**, 3901–3911 (2002).
22. Hug, N., Longman, D. & Caceres, J. F. Mechanism and regulation of the nonsense-mediated decay pathway. *Nucleic Acids Res.* **44**, 1483–1495 (2016).
23. Schafer, W. F. Genetics of egg-laying in worms. *Annu. Rev. Genet.* **40**, 487–509 (2006).
24. Sun, A. Y. & Lambie, E. J. *gon-2*, a gene required for gonadogenesis in *Caenorhabditis elegans*. *Genetics* **147**, 1077–1089 (1997).
25. Kemp, B. J., Church, D. L., Hatzold, J., Conradt, B. & Lambie, E. J. *gem-1* encodes an SLC16 monocarboxylate transporter-related protein that functions in parallel to the *gon-2* TRPM channel during gonad development in *Caenorhabditis elegans*. *Genetics* **181**, 581–591 (2009).
26. Cho, K. F. et al. Split-TurboID enables contact-dependent proximity labeling in cells. *Proc. Natl. Acad. Sci. USA* **117**, 12143–12154 (2020).
27. Medrano, E. & Collins, K. M. Muscle-directed mechanosensory feedback activates egg-laying circuit activity and behavior in *Caenorhabditis elegans*. *Curr. Biol.* **33**, 2330–2339 e2338 (2023).
28. Conradt, B. & Horvitz, H. R. The *C. elegans* protein EGL-1 is required for programmed cell death and interacts with the Bcl-2-like protein CED-9. *Cell* **93**, 519–529 (1998).
29. Sze, J. Y., Victor, M., Loer, C., Shi, Y. & Ruvkun, G. Food and metabolic signalling defects in *a Caenorhabditis elegans* serotonin-synthesis mutant. *Nature* **403**, 560–564 (2000).
30. Trent, C., Tsung, N. & Horvitz, H. R. Egg-laying defective mutants of the nematode *Caenorhabditis elegans*. *Genetics* **104**, 619–647 (1983).
31. Emtage, L. et al. IRK-1 potassium channels mediate peptidergic inhibition of *Caenorhabditis elegans* serotonin neurons via a G(o) signaling pathway. *J. Neurosci.* **32**, 16285–16295 (2012).
32. Take-uchi, M., Kobayashi, Y., Kimura, K. D., Ishihara, T. & Katsura, I. FLR-4, a novel serine/threonine protein kinase, regulates defecation rhythm in *Caenorhabditis elegans*. *Mol. Biol. Cell* **16**, 1355–1365 (2005).
33. Sommermann, E. M., Strohmaier, K. R., Maduro, M. F. & Rothman, J. H. Endoderm development in *Caenorhabditis elegans*: the synergistic action of ELT-2 and -7 mediates the specification → differentiation transition. *Dev. Biol.* **347**, 154–166 (2010).
34. Huang, Y. C. et al. A single neuron in *C. elegans* orchestrates multiple motor outputs through parallel modes of transmission. *Curr. Biol.* **33**, 4430–4445 e4436 (2023).
35. Dana, H. et al. High-performance calcium sensors for imaging activity in neuronal populations and microcompartments. *Nat. Methods* **16**, 649–657 (2019).
36. Balamurugan, K., Ashokkumar, B., Moussaif, M., Sze, J. Y. & Said, H. M. Cloning and functional characterization of a folate transporter from the nematode *Caenorhabditis elegans*. *Am. J. Physiol.* **293**, C670–C681 (2007).
37. Fanet, H., Capuron, L., Castanon, N., Calon, F. & Vancassel, S. Tetrahydrobioterin (BH4) pathway: from metabolism to neuropsychiatry. *Curr. Neuropharmacol.* **19**, 591–609 (2021).
38. Gao, L., Chalupsky, K., Stefani, E. & Cai, H. Mechanistic insights into folic acid-dependent vascular protection: dihydrofolate reductase (DHFR)-mediated reduction in oxidant stress in endothelial cells and angiotensin II-infused mice: a novel HPLC-based fluorescent assay for DHFR activity. *J. Mol. Cell. Cardiol.* **47**, 752–760 (2009).
39. Chalupsky, K., Kracun, D., Kanchev, I., Bertram, K. & Gorlach, A. Folic acid promotes recycling of tetrahydrobiopterin and protects against hypoxia-induced pulmonary hypertension by recoupling endothelial nitric oxide synthase. *Antioxid. Redox Signal.* **23**, 1076–1091 (2015).
40. Berridge, M. J., Bootman, M. D. & Roderick, H. L. Calcium signalling: dynamics, homeostasis and remodelling. *Nat. Rev. Mol. Cell Biol.* **4**, 517–529 (2003).
41. Ma, Z. & Freeman, M. R. TrpML-mediated astrocyte microdomain Ca2+ transients regulate astrocyte-tracheal interactions. *Elife* **9**, e58952 (2020).
42. Teramoto, T., Lambie, E. J. & Iwasaki, K. Differential regulation of TRPM channels governs electrolyte homeostasis in the *C. elegans* intestine. *Cell Metab.* **1**, 343–354 (2005).

43. Xing, J., Yan, X., Estevez, A. & Strange, K. Highly $Ca2^+$-selective TRPM channels regulate IP3-dependent oscillatory $Ca2^+$ signaling in the *C. elegans* intestine. *J. Gen. Physiol.* **131**, 245–255 (2008).
44. Inoue, K., Xiong, Z. G. & Ueki, T. The TRPM7 channel in the nervous and cardiovascular systems. *Curr. Protein Pept. Sci.* **21**, 985–992 (2020).
45. Krapivinsky, G., Mochida, S., Krapivinsky, L., Cibulsky, S. M. & Clapham, D. E. The TRPM7 ion channel functions in cholinergic synaptic vesicles and affects transmitter release. *Neuron* **52**, 485–496 (2006).
46. Turlova, E. et al. TRPM7 regulates axonal outgrowth and maturation of primary hippocampal neurons. *Mol. Neurobiol.* **53**, 595–610 (2016).
47. Low, S. E. et al. TRPM7 is required within zebrafish sensory neurons for the activation of touch-evoked escape behaviors. *J. Neurosci.* **31**, 11633–11644 (2011).
48. Koelle, M. R. & Horvitz, H. R. EGL-10 regulates G protein signaling in the *C. elegans* nervous system and shares a conserved domain with many mammalian proteins. *Cell* **84**, 115–125 (1996).
49. Brundage, L. et al. Mutations in *a C. elegans* Gqalpha gene disrupt movement, egg laying, and viability. *Neuron* **16**, 999–1009 (1996).
50. Blakley, R. L. (ed) *The Biochemistry of Folic Acid and Related Pteridines* (North-Holland Publishing Company, Amsterdam, 1969).
51. Balashova, O. A. et al. Noncanonical function of folate through folate receptor 1 during neural tube formation. *Nat. Commun.* **15**, 1642 (2024).
52. Gennet, N., Tamburini, C., Nan, X. & Li, M. FolR1: a novel cell surface marker for isolating midbrain dopamine neural progenitors and nascent dopamine neurons. *Sci. Rep.* **6**, 32488 (2016).
53. Dag, U. et al. Dissecting the functional organization of the *C. elegans* serotonergic system at whole-brain scale. *Cell* **186**, 2574–2592 e2520 (2023).
54. Bifsha, P., Yang, J., Fisher, R. A. & Drouin, J. Rgs6 is required for adult maintenance of dopaminergic neurons in the ventral substantia nigra. *PLoS Genet.* **10**, e1004863 (2014).
55. Hui, M. & Beier, K. T. Defining the interconnectivity of the medial prefrontal cortex and ventral midbrain. *Front. Mol. Neurosci.* **15**, 971349 (2022).
56. Brenner, S. The genetics of *Caenorhabditis elegans*. *Genetics* **77**, 71–94 (1974).
57. Fu, B. X., Hansen, L. L., Artiles, K. L., Nonet, M. L. & Fire, A. Z. Landscape of target:guide homology effects on Cas9-mediated cleavage. *Nucleic Acids Res.* **42**, 13778–13787 (2014).
58. Paix, A. et al. Precision genome editing using synthesis-dependent repair of Cas9-induced DNA breaks. *Proc. Natl. Acad. Sci. USA* **114**, E10745–E10754 (2017).
59. VanLeuven, A. J., Park, S., Menke, D. B. & Lauderdale, J. D. A PAGE screening approach for identifying CRISPR-Cas9-induced mutations in zebrafish. *Biotechniques* **64**, 275–278 (2018).
60. Frokjaer-Jensen, C., Davis, M. W., Ailion, M. & Jorgensen, E. M. Improved Mos1-mediated transgenesis in *C. elegans*. *Nat. Methods* **9**, 117–118 (2012).
61. Frokjaer-Jensen, C. et al. An abundant class of non-coding DNA can prevent stochastic gene silencing in the *C. elegans* germline. *Cell* **166**, 343–357 (2016).
62. El Mouridi, S. et al. Reliable CRISPR/Cas9 genome engineering in *Caenorhabditis elegans* using a single efficient sgRNA and an easily recognizable phenotype. *G3 (Bethesda)* **7**, 1429–1437 (2017).
63. Hostettler, L. et al. The bright fluorescent protein mNeonGreen facilitates protein expression analysis in vivo. *G3 (Bethesda)* **7**, 607–615 (2017).
64. Hussey, R. et al. Oxygen-sensing neurons reciprocally regulate peripheral lipid metabolism via neuropeptide signaling in *Caenorhabditis elegans*. *PLoS Genet.* **14**, e1007305 (2018).
65. Bruinsma, J. J., Jirakulaporn, T., Muslin, A. J. & Kornfeld, K. Zinc ions and cation diffusion facilitator proteins regulate Ras-mediated signaling. *Dev. Cell* **2**, 567–578 (2002).
66. Mello, C. & Fire, A. in *Caenorhabditis elegans: Modern Biological Analysis of an Organism* Vol. 48 *Methods in Cell Biology* (eds H. F. Epstein & D. C. Shakes) 451-482 (Academic Press, San Diego, 1995).
67. Frokjaer-Jensen, C. et al. Random and targeted transgene insertion in *Caenorhabditis elegans* using a modified Mos1 transposon. *Nat. Methods* **11**, 529–534 (2014).
68. Stover, P. & Schirch, V. Synthesis of (6S)-5-formyltetrahydropteroylpolyglutamates and interconversion to other reduced pteroylpolyglutamate derivatives. *Anal. Biochem.* **202**, 82–88 (1992).
69. Sulston, J. & Hodgkin, J. in *The Nematode Caenorhabditis elegans* (ed W. B. Wood) 587–606 (Cold Spring Harbor Laboratory, Plainview, 1988).
70. Loer, C. M. & Kenyon, C. J. Serotonin-deficient mutants and male mating behavior in the nematode *Caenorhabditis elegans*. *J. Neurosci.* **13**, 5407–5417 (1993).
71. Shakes, D. C., Miller, D. M. 3rd & Nonet, M. L. Immunofluorescence microscopy. *Methods Cell Biol.* **107**, 35–66 (2012).

Acknowledgements

We thank Jherek Swanger, Eric J. Lambie, and Stephen A. Vella for the research reagents. We thank Kamila V. Artemenko, Sidney Nguyen, and Emma G. Tyrone for assistance with video quantitation and presentation. We thank Daichi Kamiyama for constructive comments on the manuscript. Some strains were provided by the CGC, which is funded by the NIH Office of Research Infrastructure Programs (P40 OD010440). We acknowledge the assistance of the Biomedical Microscopy Core at the University of Georgia with imaging. This research was funded by a grant from the NIH National Institute of General Medical Sciences (NIGMS): R01GM134359 (ETK).

Author contributions

E.T.K. and J.S. acquired funding and conceived the experiments. R.S.P. and S.A.M. analyzed egg laying. B.L.A.-B., M.G.H., and E.T.K. analyzed Ca^{2+} levels in neurons. J.B.S., N.K., and F.Z.N. analyzed protein interactions. F.Z.N., A.C.W., and B.L.A.-B. analyzed expression patterns and protein localization. R.N.K. and M.G.H. analyzed animal motion. D.G. analyzed serotonin levels. A.K.G. analyzed mRNA levels. E.T.K. wrote the manuscript with contributions from all authors. All authors read and approved the final manuscript.

Competing interests

The authors declare no competing interests.

Additional information

Supplementary information The online version contains supplementary material available at https://doi.org/10.1038/s41467-024-52738-z.

Correspondence and requests for materials should be addressed to Edward T. Kipreos.

Peer review information *Nature Communications* thanks Kevin Collins, Jürgen König, and the other, anonymous, reviewer(s) for their contribution to the peer review of this work. A peer review file is available.